Lattice-Reduction-Aided and Integer-Forcing Equalization

Structures, Criteria, Factorization, and Coding

Other titles in Foundations and Trends® in Communications and Information Theory

Group Testing: An Information Theory Perspective
Matthew Aldridge, Oliver Johnson and Jonathan Scarlett
ISBN: 978-1-68083-596-0

Sparse Regression Codes
Ramji Venkataramanan, Sekhar Tatikonda and Andrew Barron
ISBN: 978-1-68083-580-9

Fundamentals of Index Coding
Fatemeh Arbabjolfaei and Young-Han Kim
ISBN: 978-1-68083-492-5

Community Detection and Stochastic Block Models
Emmanuel Abbe
ISBN: 978-1-68083-476-5

Lattice-Reduction-Aided and Integer-Forcing Equalization

Structures, Criteria, Factorization, and Coding

Robert F.H. Fischer
Ulm University
robert.fischer@uni-ulm.de

Sebastian Stern
Ulm University
sebastian.stern@uni-ulm.de

Johannes B. Huber
Friedrich-Alexander-Universität Erlangen-Nürnberg
johannes.huber@fau.de

the essence of knowledge
Boston — Delft

Foundations and Trends® in Communications and Information Theory

Published, sold and distributed by:
now Publishers Inc.
PO Box 1024
Hanover, MA 02339
United States
Tel. +1-781-985-4510
www.nowpublishers.com
sales@nowpublishers.com

Outside North America:
now Publishers Inc.
PO Box 179
2600 AD Delft
The Netherlands
Tel. +31-6-51115274

The preferred citation for this publication is

R. F.H. Fischer, S. Stern, and J. B. Huber. *Lattice-Reduction-Aided and Integer-Forcing Equalization*. Foundations and Trends® in Communications and Information Theory, vol. 16, no. 1–2, pp. 1–155, 2019.

ISBN: 978-1-68083-645-5

Foundations and Trends® in Communications and Information Theory

Volume 16, Issue 1–2, 2019

Editorial Board

Editorial Scope

Topics

Foundations and Trends® in Communications and Information Theory publishes survey and tutorial articles in the following topics:

- Coded modulation
- Coding theory and practice
- Communication complexity
- Communication system design
- Cryptology and data security
- Data compression
- Data networks
- Demodulation and Equalization
- Denoising
- Detection and estimation
- Information theory and statistics
- Information theory and computer science
- Joint source/channel coding
- Modulation and signal design
- Multiuser detection
- Multiuser information theory
- Optical communication channels
- Pattern recognition and learning
- Quantization
- Quantum information processing
- Rate-distortion theory
- Shannon theory
- Signal processing for communications
- Source coding
- Storage and recording codes
- Speech and Image Compression
- Wireless Communications

Information for Librarians

Foundations and Trends® in Communications and Information Theory, 2019, Volume 16, 4 issues. ISSN paper version 1567-2190. ISSN online version 1567-2328 . Also available as a combined paper and online subscription.

Contents

Lattice-Reduction-Aided and Integer-Forcing Equalization

Robert F.H. Fischer[1], Sebastian Stern[2], and Johannes B. Huber[3]

[1] *Ulm University; robert.fischer@uni-ulm.de*
[2] *Ulm University; sebastian.stern@uni-ulm.de*
[3] *Friedrich-Alexander-Universität Erlangen-Nürnberg; johannes.huber@fau.de*

ABSTRACT

In this monograph, a tutorial review of lattice-reduction-aided (LRA) and integer-forcing (IF) equalization approaches in MIMO communications is given. Both methods have in common that integer linear combinations are decoded; the remaining integer interference is resolved subsequently. The aim is to enlighten similarities and differences of both approaches. The various criteria for selecting the integer linear combinations available in the literature are summarized in a unified way. Thereby, we clearly distinguish between the criteria according to which the non-integer equalization part is optimized and those, which are inherently considered in the applied lattice algorithms, i.e., constraints on the integer equalization part. The demands on the signal constellations and coding schemes are discussed in detail. We treat LRA/IF approaches for receiver-side linear equalization and decision-feedback equalization, as well as transmitter-side linear preequalization and precoding.

Robert F.H. Fischer, Sebastian Stern, and Johannes B. Huber (2019), "Lattice-Reduction-Aided and Integer-Forcing Equalization", Foundations and Trends® in Communications and Information Theory: Vol. 16, No. 1–2, pp. 1–155. DOI: 10.1561/0100000100.

1

Introduction

Primarily, in the early days of communication and information theory point-to-point transmission between a single transmitter and a single receiver was studied, cf. the famous "Fig. 1" in [110]. Soon it was realized that gains can be achieved by handling users jointly, leading to the development of the the concept of the *multiple-access channel (MAC)* in the 1970s [2, 79]. Thereby, many users are transmitting signals simultaneously with no separation in time, frequency, or space to a central receiver which has to separate out the individual messages from the noisy mixture of the users' signals. At the same time, the dual concept of the *broadcast channel* [19] was introduced: a central transmitter supplies several users with their individual messages.

Around the same time, the concept of *multiple-input/multiple-output (MIMO)* transmission was devised, e.g., [75, 28, 104]. Here, a number of signals is transmitted in parallel and a number of interfered and noisy signals is received in parallel, i.e., the dimension *space* is utilized. The breakthrough of the MIMO concept happened in the 1990s, where it was applied to enhance the performance of wireless communications [124]; both to increase the data rate (multiplexing gain) and the reliability (diversity gain) [127]. Most prominently, the *Bell*

Laboratories layered space-time (BLAST) system has to be mentioned [46, 52].

Since then, the design of joint receivers which observe multiple versions of noisy superpositions of the signals transmitted in parallel is an important field of research. Initially, concepts well-known from the equalization of linear, dispersive (single-input/single-output) channels were transferred to the MIMO setting, cf. [31, Table E.1]. Because *maximum-likelihood detection (MLD)* usually requires too much complexity even if implemented using the *sphere decoder* [1], cf. also [87], suboptimal schemes are of interest.

The simplest approach for handling the interference in MIMO communications is to apply *linear equalization (LE)*, which can either be optimized according to the *zero-forcing (ZF)* or the *minimum mean-squared error (MMSE)* criterion. Improvements can be achieved when employing *decision-feedback equalization (DFE)*, which is also known under the term *successive interference cancellation (SIC)*, and is used in BLAST. However, the performance of both approaches is poor—in particular, the achievable diversity order is significantly smaller than it would be possible using MLD which fully exploits the MIMO channel's diversity [127].

Since almost two decades, low-complexity but well-performing approaches are available. These *lattice-reduction-aided (LRA)* techniques, e.g., [151, 139], require some initial effort to calculate the equalizer front-end but then have the same low complexity per time step as LE or DFE. It was proven that LRA schemes achieve the optimal diversity order [122]. As the name suggests, the mathematical principle behind LRA equalization is *lattice reduction*, e.g., [148]. The channel is interpreted as the generator matrix of the regular arrangement—the *lattice* [16]—of the signal points seen at the receiver. Since any lattice can be given in an infinite number of bases, a "convenient" one can be chosen—equalization is done based on a change to a suited basis. As a consequence of this change of basis, not the users' signals are detected/decoded initially but *integer linear combinations* thereof [38]. An integer matrix $\boldsymbol{Z}$ collects the linear factors and describes the change of basis. In a final step, after decoding, this change of basis (the action of $\boldsymbol{Z}$) is reversed; the integer interference has to be resolved.

Recently, the concept of *integer-forcing (IF)* equalization for joint linear equalization was proposed in [154]. This approach, originating from *compute-and-forward* relaying schemes [88], and related to algebraic physical-layer network coding [30], is not only advantageous in MIMO systems, but in multiple-access scenarios in general, e.g., [95]. Meanwhile, various extensions of the IF philosophy exist, e.g., successive integer-forcing [94] or integer-forcing source coding [96].

The term "LRA" can be interpreted as a channel-oriented view—it emphasizes the mathematical tool applied to the channel matrix. In contrast, the denomination "IF" is signal-oriented—it highlights the main operation on the signals.

As the name suggests, the main idea in IF is to force the interference to be an integer linear combination of the other users' signals. In this regard, LRA and IF techniques coincide. However, LRA and IF receivers differ in the way the integer interference is handled, i.e., how the integer matrix $\boldsymbol{Z}$ characterizing the linear combinations is inverted, cf. [42]. Moreover, rooted in the way how the integer interference is resolved, the mathematical principle of lattice reduction is weakened to a more general lattice problem in IF relaxing the constraints on $\boldsymbol{Z}$ present in the initial proposal of LRA. Finally, in contrast to LRA schemes which are usually assume uncoded transmission, IF schemes were directly proposed as coded schemes. In IF schemes, a strong coupling between equalization and decoding exists, leading to significant constraints on the signal constellations. In our view, the restriction to prime-field arithmetic and matched constellations in IF is the much more important conceptional difference between LRA and IF than that of studying uncoded and coded transmission, respectively.

Meanwhile, a huge number of papers dealing with various aspects of IF equalization were published. In particular, the calculation of the receiver frontend and the code construction are of interest, see, e.g., [92, 103, 23, 116, 92, 42, 137, 11], to name only a few. Thereby, the fundamental difference between the LRA and IF philosophy is often blurred. Many equalization and lattice factorization approaches are not limited to IF but can also be applied in LRA receivers. Indeed, the invention of IF schemes has sparked a rethinking of the LRA approach.

Besides joint receiver-side equalization in the MIMO MAC (typically the uplink in mobile communications), the joint transmitter-side preequalization in MIMO *broadcast channels (BC)* (downlink) is of importance. Basically, the two scenarios and respective operations/equalization structures are dual to each other. For linear equalization and DFE/precoding this fact is summarized in the famous *uplink/downlink duality* [108, 130, 131, 152, 74].

Of course, this duality holds for LRA and IF schemes as well. LRA precoding was introduced in [139, 143, 119]. IF schemes for the downlink were proposed in [62] and [56]. Meanwhile, a (weakened) uplink/downlink duality was proved for the IF architecture [57].

In this monograph, a tutorial review of the LRA and IF approaches in MIMO communications is given. The aim is to enlighten the similarities and differences of both approaches. The various criteria for selecting the integer linear combinations available in the literature are summarized in a unified way. Thereby, we clearly distinguish between the criteria according to which the equalization part is optimized and those, which are inherently considered in the applied lattice algorithms. The demands on the signal constellations and coding schemes are discussed in detail. We treat LRA/IF approaches for receiver-side linear equalization and DFE, as well as transmitter-side linear preequalization and precoding.

The work is organized as follows: In Chapter 2 the system model is introduced and classical equalization schemes are briefly reviewed to establish the basis for the subsequent presentation. The equalization task is discussed in detail in Chapter 3. We categorize the different criteria available in the literature for adjusting the equalization part, the different constraints on the matrix $\boldsymbol{Z}$, and the related type of lattice problem which has to be solved for calculating $\boldsymbol{Z}$. In Chapter 4, the demands on the coding schemes and signal constellations in LRA and IF receivers are pointed out. Chapter 5 contrasts the LRA and IF philosophy when DFE is applied and in Chapter 6 transmitter-side LRA and IF precoding are analyzed. A brief summary and a final comparison are given in Chapter 7. For completeness a short review on lattices and lattice algorithms is compiled in Appendix A. To enhance readability, in Appendix D the notation used throughout the monograph is collected as a reference. Finally, in Appendix C some practical issues concerning offsets in constellations and handling of non-valid decoding results are collected.

Table 7.1: Comparison of LRA and IF equalization.

Lattice-Reduction-Aided Equalization	Integer-Forcing Equalization
denomination	
channel-oriented	signal-oriented
best suited for	
joint receiver / transmitter	distributed antenna systems
decoding of integer linear combinations	
of transmit words in signal space	of source words (modulo p)
treat integer interference over	
$\mathbb{G} = \mathbb{Z} + \mathrm{j}\mathbb{Z}$ via $\boldsymbol{Z}^{-1}$	$\mathbb{F}_p$ via $\boldsymbol{\mathfrak{Z}}^{-1}$
constraint on signal constellation, mapping, and coding	
often considered uncoded signal points drawn from a lattice (relaxed for MLC) no restriction on the cardinality	incorporation of coding match arithmetic in $\mathbb{R}$ (or $\mathbb{C}$) and $\mathbb{F}_p$ p-ary prime constellation required
integer matrix $\boldsymbol{Z} \in \mathbb{G}^{K \times K}$	
(initially $\lvert\det(\boldsymbol{Z})\rvert = 1$ forced — *SBP*) $\mathrm{rank}(\boldsymbol{Z}) = K$ sufficient — *SIVP*	$\mathrm{rank}(\boldsymbol{\mathfrak{Z}}) = K$; *SIVP*

Appendices

A

Lattices, Lattice Problems, and Algorithms

This appendix collects the most important properties of lattices, the problems of finding a so-called *reduced basis* or a set of *shortest independent vectors* for a given lattice, and related algorithms. Thereby, we restrict ourselves to *complex-valued lattices* and algorithms directly operating on complex lattices rather than the real-valued equivalent. Operating in the equivalent complex baseband domain of signals where the signal point lattice is equal to the *Gaussian integers*, this is a suited approach.

A.1 Lattices

Let an $N \times K$ *generator* or *basis matrix* $\boldsymbol{G} = [\boldsymbol{g}_1, \ldots, \boldsymbol{g}_K] \in \mathbb{C}^{N \times K}$, which consists of $K \in \mathbb{N}$ *linearly independent basis vectors* $\boldsymbol{g}_k \in \mathbb{C}^N$, $N \geq K$, $N \in \mathbb{N}$, be given. A complex-valued N-dimensional *lattice* of rank K is defined as

$$\boldsymbol{\Lambda}(\boldsymbol{G}) \stackrel{\text{def}}{=} \{\boldsymbol{\lambda} = \boldsymbol{G}\boldsymbol{u} \mid \boldsymbol{u} \in \mathbb{G}^K\} \,. \tag{A.1}$$

For real lattices, $\boldsymbol{G}$ has to be real and $\mathbb{G} = \mathbb{Z} + \mathrm{j}\mathbb{Z}$ is replaced by $\mathbb{Z}$.

If the particular generator matrix is immaterial, we simply write $\boldsymbol{\Lambda}$ for the lattice.

A complex lattice is a discrete set of points in $\mathbb{C}^N$ which has group structure under ordinary vector addition [153, 31]. It is spanned by the basis vectors $\boldsymbol{g}_k$, i.e., the lattice points $\boldsymbol{\lambda} \in \boldsymbol{\Lambda}$ are (Gaussian) integer linear combinations of the basis vectors and the set $\{\boldsymbol{g}_1, \dots, \boldsymbol{g}_K\}$ is the *basis* of the lattice.[1] Noteworthy, any lattice contains the origin $\boldsymbol{\lambda} = \mathbf{0} = [0, \dots, 0]^\mathsf{T}$ as a valid point.

To each lattice point a *Voronoi region* can be associated. It is defined as the set of points in $\mathbb{C}^N$, which are closer to the considered point than to any other lattice point. Here, we are only interested in the Voronoi region w.r.t. the origin and have (ties have to be resolved in a suited way; $||\cdot||$: Euclidean norm)

$$\mathcal{R}_\mathrm{V}(\boldsymbol{\Lambda}) \overset{\text{def}}{=} \{\boldsymbol{x} \in \mathbb{C} \;\mid\; ||\boldsymbol{x}|| \leq ||\boldsymbol{x} - \boldsymbol{\lambda}||,\ \forall \boldsymbol{\lambda} \in \boldsymbol{\Lambda} \setminus \{\mathbf{0}\}\} \,. \tag{A.2}$$

Given a lattice $\boldsymbol{\Lambda}$ with generator matrix $\boldsymbol{G}$, the *dual lattice*, denoted by $\boldsymbol{\Lambda}^\perp$, is the set of vectors $\boldsymbol{\lambda}^\perp \in \mathbb{C}^N$ in the linear span of the columns $\boldsymbol{g}_k$ of $\boldsymbol{G}$, such that the scalar product between any lattice point from $\boldsymbol{\Lambda}$ and $\boldsymbol{\Lambda}^\perp$ is an (Gaussian) integer; mathematically

$$\boldsymbol{\Lambda}^\perp \overset{\text{def}}{=} \{\boldsymbol{\lambda}^\perp \in \mathbf{span}(\boldsymbol{G}) \mid \forall \boldsymbol{\lambda} \in \boldsymbol{\Lambda}\ ,\ \boldsymbol{\lambda}^\mathsf{H} \boldsymbol{\lambda}^\perp \in \mathbb{G}\} \,. \tag{A.3}$$

The generator matrix $\boldsymbol{G}^\perp$ of the dual lattice is given by [16]

$$\boldsymbol{G}^\perp \overset{\text{def}}{=} \boldsymbol{G}(\boldsymbol{G}^\mathsf{H}\boldsymbol{G})^{-1} \;=\; (\boldsymbol{G}^+)^\mathsf{H} \,, \tag{A.4}$$

where $\boldsymbol{G}^+ \overset{\text{def}}{=} (\boldsymbol{G}^\mathsf{H}\boldsymbol{G})^{-1}\boldsymbol{G}^\mathsf{H}$ is the Moore–Penrose left inverse of $\boldsymbol{G}$.

[1]We will often use the terms generator/basis matrix and basis synonymously, knowing that the matrix, contrary to the set, assumes as particular ordering of the basis vectors.

A.2 Lattice Problems

Given a lattice $\boldsymbol{\Lambda}$ (via its generator matrix $\boldsymbol{G}$), fundamental problems can be stated. First, one is often interested in the question which lattice point is closest (w.r.t. Euclidean norm) to a given (non-lattice) point $\boldsymbol{x} \in \mathbb{C}^N$, the so-called "*closest point problem*". This is also denoted as "*lattice quantization*" and is mathematically defined as

$$\hat{\boldsymbol{\lambda}} = \mathrm{Q}_{\boldsymbol{\Lambda}}(\boldsymbol{x}) \stackrel{\text{def}}{=} \operatorname*{argmin}_{\boldsymbol{\lambda} \in \boldsymbol{\Lambda}} ||\boldsymbol{x} - \boldsymbol{\lambda}||^2 . \tag{A.5}$$

Next, the knowledge about the shortest vector (except $\mathbf{0}$) of a lattice $\boldsymbol{\Lambda}$, called "*shortest vector problem*", is sometimes of importance. We have

$$\boldsymbol{\lambda}_{\text{shortest}} \stackrel{\text{def}}{=} \operatorname*{argmin}_{\boldsymbol{\lambda} \in \boldsymbol{\Lambda} \setminus \{\mathbf{0}\}} ||\boldsymbol{\lambda}||^2 . \tag{A.6}$$

An important fact about lattices is that the generator matrix is not unique. Let $\boldsymbol{Z} \in \mathbb{G}^{K \times K}$ with $|\det(\boldsymbol{Z})| = 1$, i.e., $\boldsymbol{Z}$ is a so-called *integer unimodular matrix*. Then, $\{\boldsymbol{Zu} \mid \boldsymbol{u} \in \mathbb{G}^K\} = \mathbb{G}^K$, or in short $\boldsymbol{Z}\mathbb{G}^K = \mathbb{G}^K$. Graphically, the transformation of the (Gaussian) integers $\mathbb{G}$ by a unimodular matrix is identical to the (Gaussian) integers itself. Consequently, we have

$$\{\boldsymbol{Gu} \mid \boldsymbol{u} \in \mathbb{G}^K\} = \{\boldsymbol{GZu} \mid \boldsymbol{u} \in \mathbb{G}^K\} , \tag{A.7}$$

hence $\boldsymbol{G}$ and $\boldsymbol{GZ}$ span the same lattice.

This property of lattices gives rise to some important problems, most prominently the question of a "suited" or "desired" basis ("*lattice basis reduction*" or "*shortest basis problem*" (SBP)). In contrast, the "*shortest independent vector problem*" (SIVP) asks for K linearly independent vectors from the lattice such that the longest is as short as possible; its stronger form is called "*successive minima problem*" (SMP).

Subsequently, we define these problems and briefly review suited algorithms for solving these problems. To this end, we first have to define the Gram–Schmidt orthogonalization.

A.3 Gram–Schmidt Orthogonalization

Any $N \times K$ matrix $\boldsymbol{G}$, $N \geq K$, can be decomposed into the form [53]

$$\boldsymbol{G} = \boldsymbol{G}^{\circ}\boldsymbol{R} \,, \tag{A.8}$$

where $\boldsymbol{G}^{\circ} = [\boldsymbol{g}_1^{\circ}, \ldots, \boldsymbol{g}_K^{\circ}] \in \mathbb{C}^{N \times K}$ has *orthogonal columns* $\boldsymbol{g}_k^{\circ}$, i.e., $(\boldsymbol{g}_i^{\circ})^{\mathsf{H}} \boldsymbol{g}_j^{\circ} = 0$, $i \neq j$, and $\boldsymbol{R} \in \mathbb{C}^{K \times K}$ is upper triangular with unit main diagonal.[2]

The process of calculating $\boldsymbol{G}^{\circ}$ and $\boldsymbol{R}$ from $\boldsymbol{G}$ is called *Gram–Schmidt procedure*.[3] It operates successively and calculates

$$\boldsymbol{g}_k^{\circ} = \boldsymbol{g}_k - \sum_{l=1}^{k-1} r_{l,k} \, \boldsymbol{g}_l^{\circ} \,, \quad k = 1, \ldots, K \,, \tag{A.9}$$

where the (upper triangular) coefficients of $\boldsymbol{R}$ are given by

$$r_{l,k} = \frac{(\boldsymbol{g}_l^{\circ})^{\mathsf{H}} \boldsymbol{g}_k^{\circ}}{||\boldsymbol{g}_l^{\circ}||^2} \,, \quad l = 1, \ldots, k \,. \tag{A.10}$$

A.4 Shortest Independent Vector Problem

In some situations, K linearly independent vectors from the lattice $\boldsymbol{\Lambda}$ are required. However, usually not arbitrary vectors are accepted—typically they should be as short as possible, meaning their norms should be small. For that we require a reference what small is. This is given by *Minkowski's successive minima*.

A.4.1 Successive Minima

The k^{th} *successive minimum* $\rho_k(\boldsymbol{\Lambda})$, $k = 1, \ldots, K$, of $\boldsymbol{\Lambda}$ is defined as [77]

$$\rho_k(\boldsymbol{\Lambda}) \stackrel{\text{def}}{=} \inf \left\{ \varrho_k \mid \dim \left(\mathbf{span} \left(\boldsymbol{\Lambda} \cap \mathcal{B}(\varrho_k) \right) \right) = k \right\} , \tag{A.11}$$

[2] Normalizing $\boldsymbol{g}_k^{\circ}$ to unit norm and incorporating the respective normalization factors into $\boldsymbol{R}$ by scaling of the row, a *QR decomposition* is obtained ($\boldsymbol{G}^{\circ}$ would then be a unitary matrix).

[3] In the decomposition (A.8) a reordering of the columns of $\boldsymbol{G}$ (by a permutation matrix) may be allowed; this adds a pivoting step in the Gram–Schmidt procedure.

where $\mathcal{B}(\varrho) \stackrel{\text{def}}{=} \{\boldsymbol{x} \in \mathbb{C}^N \mid ||\boldsymbol{x}|| \leq \varrho\}$ is the N-dimensional ball (over $\mathbb{C}$) with radius ϱ centered at the origin and $\dim(\mathbf{span}(\cdot))$ denotes the dimension of the linear span of the given set of vectors. Graphically, ρ_k is the smallest radius for which the ball $\mathcal{B}$ contains k linearly independent lattice vectors.

A.4.2 Shortest Independent Vector Problem (SIVP)

Given a lattice $\boldsymbol{\Lambda}$ of rank K, the SIVP asks for a set $\mathcal{G} = \{\boldsymbol{\lambda}_1, \ldots, \boldsymbol{\lambda}_K\}$ of K linearly independent lattice vectors with $||\boldsymbol{\lambda}_k|| \leq ||\boldsymbol{\lambda}_\kappa||$, $k < \kappa$, such that the maximal norm of these vectors is not larger than the K^{th} minimum. Mathematically, the SIVP reads

$$||\boldsymbol{\lambda}_k|| \leq \rho_K(\boldsymbol{\Lambda}) \;, \quad k = 1, \ldots, K \;, \tag{A.12}$$

or, since $\boldsymbol{\lambda}_K$ cannot be shorter than the K^{th} successive minimum,

$$\max_{k=1,\ldots,K} ||\boldsymbol{\lambda}_k|| = \rho_K(\boldsymbol{\Lambda}) \;. \tag{A.13}$$

A.4.3 Successive Minima Problem (SMP)

In the SIVP, the norms of the shorter vectors are irrelevant. Contrary, we now request a set $\mathcal{G} = \{\boldsymbol{\lambda}_1, \ldots, \boldsymbol{\lambda}_K\}$ of K linearly independent lattice vectors, such that the norm of the k^{th} vector is identical to the k^{th} minimum. Mathematically, the SMP reads

$$||\boldsymbol{\lambda}_k|| = \rho_k(\boldsymbol{\Lambda}) \;, \quad k = 1, \ldots, K \;. \tag{A.14}$$

Apparently, the SMP is a stronger form and provides a particular solution to the SIVP.

A.4.4 Algorithms

Efficient algorithms for solving not only the real-valued but also the complex-valued version of the (C)SMP (and hence the (C)SIVP) have been proposed, e.g., [23, 42, 137].

A.5 Lattice Basis Reduction

In a number of applications, given a lattice $\boldsymbol{\Lambda}(\boldsymbol{G})$, a generator matrix $\boldsymbol{G}_\mathrm{r} = [\boldsymbol{g}_{\mathrm{r},1}, \ldots, \boldsymbol{g}_{\mathrm{r},K}]$ is requested, which spans the same lattice, i.e., $\boldsymbol{\Lambda}(\boldsymbol{G}_\mathrm{r}) = \boldsymbol{\Lambda}(\boldsymbol{G})$, and where the basis vectors are as short as possible. This problem is called *shortest basis problem (SBP)* or *lattice basis reduction*; the matrix $\boldsymbol{G}_\mathrm{r}$ represents a reduced basis.

Noteworthy, the columns $\boldsymbol{g}_k$ of the generator matrix $\boldsymbol{G}$ as well as the columns $\boldsymbol{g}_{\mathrm{r},k}$ of the reduced basis $\boldsymbol{G}_\mathrm{r}$ are valid lattice points ($\boldsymbol{g}_k = \boldsymbol{G}\boldsymbol{e}_k$ and $\boldsymbol{g}_{\mathrm{r},k} = \boldsymbol{G}_\mathrm{r}\boldsymbol{e}_k$, where $\boldsymbol{e}_k$ is the k^th unit vector). Hence, $\mathcal{G}_\mathrm{r} = \{\boldsymbol{g}_{\mathrm{r},1}, \ldots, \boldsymbol{g}_{\mathrm{r},K}\}$ is a set of K short independent vectors from $\boldsymbol{\Lambda}$. As this set has to be a basis for $\boldsymbol{\Lambda}$, the SBP is a stronger form of the SIVP.

Moreover, as $\boldsymbol{g}_k, \boldsymbol{g}_{\mathrm{r},k} \in \boldsymbol{\Lambda}$, the $\boldsymbol{g}_k$s can be written as (Gaussian) integer linear combinations of the reduced basis vectors $\boldsymbol{g}_{\mathrm{r},k}$, in particular

$$\boldsymbol{G} = \boldsymbol{G}_\mathrm{r}\boldsymbol{Z} \ , \tag{A.15}$$

where $\boldsymbol{Z} \in \mathbb{G}^{K\times K}$ and (see Sec. A.2) $|\det(\boldsymbol{Z})| = 1$ (unimodular matrix), such that $\boldsymbol{Z}$ describes a change of basis. Noteworthy, as $\boldsymbol{Z}$ is a unimodular (Gaussian) integer matrix, its inverse $\boldsymbol{Z}^{-1} = \frac{\mathrm{adj}(\boldsymbol{Z})}{\det(\boldsymbol{Z})} = \mathrm{adj}(\boldsymbol{Z})$, where $\mathrm{adj}(\boldsymbol{Z})$ is the *adjugate* or *adjunct* of $\boldsymbol{Z}$ [53], is also a unimodular integer matrix.

Still, the question what is meant by "short" basis, i.e., what is accepted as valid solution, is open. Defining specific criteria on the basis vectors, different types of lattice reduction and related algorithms are obtained.

Subsequently, let the generator matrix $\boldsymbol{G} = [\boldsymbol{g}_1, \ldots, \boldsymbol{g}_K] \in \mathbb{C}^{N\times K}$ be given and let $\boldsymbol{G}^\circ = [\boldsymbol{g}_1^\circ, \ldots, \boldsymbol{g}_K^\circ]$ be the Gram–Schmidt orthogonal basis to $\boldsymbol{G}$ with upper triangular matrix $\boldsymbol{R}$.

A.5.1 Lenstra–Lenstra–Lovász Reduction

The most famous lattice-reduction algorithm is the one presented by Lenstra, Lenstra, and Lovász, in short LLL algorithm [78]. Its practicability stems from conveniently defined criteria when a basis is said to be LLL-reduced. The initial algorithm treated real-valued lattices—an extension to complex-valued lattices was given in [48].

The basis/generator matrix is called *(C)LLL-reduced* with parameter $0.5 < \delta \le 1$, if [48]

i) *Size Reduction:* for $1 \le l < k \le K$ it holds

$$|\mathrm{Re}\{r_{l,k}\}| \le 0.5 \quad \text{and} \quad |\mathrm{Im}\{r_{l,k}\}| \le 0.5 \,, \tag{A.16}$$

ii) *Lovász Condition:* for $k = 2, \ldots, K$ it holds

$$||\boldsymbol{g}_k^\circ||^2 \ge (\delta - |r_{k-1,k}|^2)||\boldsymbol{g}_{k-1}^\circ||^2 \,. \tag{A.17}$$

The parameter δ controls the trade-off between "quality" of the LLL reduction and computational complexity.

For $\delta < 1$, the respective algorithm has polynomial-time complexity; usually, as in [78], $\delta = 0.75$ is chosen. For $\delta = 1$, sometimes denoted as *optimal LLL reduction*, convergence is still guaranteed mathematically [4].

Meanwhile a lot of variants and generalizations of the LLL algorithm exist, e.g., the *deep LLL* [107], the *Siegel algorithm* [112], or fixed-point implementations [83], to name only a few.

A.5.2 Hermite–Korkine–Zolotareff (HKZ) Reduction

The criterion of the *Hermite–Korkine–Zolotareff (HKZ) reduction* [76] is stronger than the LLL criterion. Now, the basis/generator matrix is called *(C)HKZ-reduced*, if [77, 72]

i) *Size Reduction* as in (A.16) is fulfilled

ii) *Shortest Vector in Sublattice:* for $k = 1, \ldots, K$, $\boldsymbol{g}_k^\circ$ is a shortest vector in the lattice $\boldsymbol{\Lambda}(\boldsymbol{G}^{(k)})$ of rank $K - k + 1$ and dimension N, which is spanned by the generator matrix $\boldsymbol{G}^{(k)} = [0, \ldots, 0, \boldsymbol{g}_k^\circ, \ldots, \boldsymbol{g}_K^\circ]\boldsymbol{R}$

To find an HKZ-reduced basis, K times a *shortest vector problem* (A.6) has to be solved. Even though the shortest vector problem itself is NP-hard, efficient practical algorithms for HKZ reduction exist, e.g., [155, 72].

A.5.3 Minkowski Reduction

One of the strongest forms of lattice reduction is that by *Minkowski (Mk)*. Here, the basis/generator matrix is called *Mk-reduced*, if [86, 155]

> for $k = 1, \ldots, K$, $\boldsymbol{g}_k$ is the shortest vector among all possible lattice points $\boldsymbol{g}'_k$, for which the set $\{\boldsymbol{g}_1, \boldsymbol{g}_2, \ldots, \boldsymbol{g}_{k-1}, \boldsymbol{g}'_k\}$ can be extended to a basis of the lattice $\boldsymbol{\Lambda}(\boldsymbol{G})$

Mk reduction can be seen as a stronger version of SMP; not only the K shortest independent lattice vectors have to be found, but they additionally have to establish a basis, i.e., the absolute value of the determinant of the associated change-of-base matrix $\boldsymbol{Z}$ has to be one.

As for the HKZ reduction, the Mk reduction is NP-hard in principle. Nevertheless, efficient practical algorithms for HKZ reduction exist,[4] e.g., [155], or that in [42] with an additional constraint on the determinant.

A.6 Algorithms Adapted to LRA/IF

Beside these mentioned generic algorithms which can immediately be used in LRA/IF schemes, algorithms specialized to the situation in LRA/IF schemes (i.e., combining the factorization criterion according to Sec. 3.3 with a desired reduction strategy) have been proposed in the literature. See, e.g., the brute-force search in [154], the algorithms in [88, 103, 102], the suboptimal algorithms in [135, 136], or the distributed approach in [62] to name only a few.

Moreover, a huge amount of variants of lattice reductions algorithms exists. See, e.g., the boosted KZ/LLL [85], the improved KZ reduction [138], LLL with deep insertions [107], Seysen's algorithm for joint reduction of a lattice and its dual lattice [111] (cf. also [147]), the parallel LLL [83], and the Siegel [112] and reverse Siegel algorithms [7].

[4]The algorithms in [155] are described for the real-valued case. In order to adapt them to the complex case, the calculation of the greatest common divisor (gcd) of real numbers has to be generalized to Gaussian integers [116].

B

Derivation of the Equalization Matrices for LRA DFE

The calculation of the optimal matrices for classical and LRA decision-feedback equalization are collected in this appendix. To enlighten the similarities and differences between the conventional and the LRA case, the BLAST approach is reviewed in detail and the equivalence of the "dual-lattice approach" (cf. Sec. 2.2.2) is proven. Based on this knowledge, the optimal factorization approach for LRA DFE is derived from general estimation principles and a generalized version of the dual lattice approach is worked out. First, in order to improve readability of the derivations, some properties of the Moore–Penrose inverse are presented.

B.1 Properties of the Moore–Penrose Inverse

It is well-known that given an $n \times m$, $n \geq m$, matrix $\boldsymbol{M}$ over $\mathbb{C}$ with full (column) rank m, the Moore–Penrose (left) inverse is given by

$$\boldsymbol{M}^{+} \stackrel{\text{def}}{=} (\boldsymbol{M}^{\mathsf{H}}\boldsymbol{M})^{-1}\boldsymbol{M}^{\mathsf{H}} . \tag{B.1}$$

For this specific type of pseudoinverse we have $\boldsymbol{M}^{+}\boldsymbol{M} = \boldsymbol{I}_m$, where $\boldsymbol{I}_m$ is the $m \times m$ identity matrix, and $(\boldsymbol{M}^{+})^{+} = \boldsymbol{M}$.

Let the *QR decomposition* of the matrix be $\boldsymbol{M} = \boldsymbol{Q}\boldsymbol{R}$, where $\boldsymbol{Q} \in \mathbb{C}^{n \times m}$ has *orthonormal columns*, i.e., $\boldsymbol{Q}^{\mathsf{H}}\boldsymbol{Q} = \boldsymbol{I}_m$, and $\boldsymbol{R}$ is $m \times m$ full-rank upper triangular with real-valued main-diagonal elements. Then, the Moore–Penrose inverse can be written as

$$\begin{aligned} \boldsymbol{M}^{+} &\stackrel{\text{def}}{=} (\boldsymbol{R}^{\mathsf{H}}\boldsymbol{Q}^{\mathsf{H}}\boldsymbol{Q}\boldsymbol{R})^{-1}\boldsymbol{R}^{\mathsf{H}}\boldsymbol{Q}^{\mathsf{H}} \\ &= \boldsymbol{R}^{-1}\boldsymbol{Q}^{\mathsf{H}} . \end{aligned} \tag{B.2}$$

We are interested in the Moore–Penrose inverse of partitioned matrices. To this end, assume that $\boldsymbol{M}_{\mathrm{a}} = [\boldsymbol{M}_1 \; \boldsymbol{M}_2]$, with $\boldsymbol{M}_1 \in \mathbb{C}^{n \times m}$, $\boldsymbol{M}_2 \in \mathbb{C}^{n \times p}$, and $m + p \leq n$, is a column-wise partitioned matrix of full (column) rank $m + p$. Its QR decomposition reads

$$[\boldsymbol{M}_1 \; \boldsymbol{M}_2] = [\boldsymbol{Q}_1 \; \boldsymbol{Q}_2] \begin{bmatrix} \boldsymbol{R}_1 & \boldsymbol{S} \\ \boldsymbol{0} & \boldsymbol{R}_2 \end{bmatrix} . \tag{B.3}$$

Applying the inverse of partitioned matrices [63], the Moore–Penrose inverse of $\boldsymbol{M}_{\mathrm{a}}$ is given by

$$\begin{aligned} \boldsymbol{M}_{\mathrm{a}}^{+} &= [\boldsymbol{M}_1 \; \boldsymbol{M}_2]^{+} \\ &= \begin{bmatrix} \boldsymbol{R}_1 & \boldsymbol{S} \\ \boldsymbol{0} & \boldsymbol{R}_2 \end{bmatrix}^{-1} [\boldsymbol{Q}_1 \; \boldsymbol{Q}_2]^{\mathsf{H}} \\ &= \begin{bmatrix} \boldsymbol{R}_1^{-1} & -\boldsymbol{R}_1^{-1}\boldsymbol{S}\boldsymbol{R}_2^{-1} \\ \boldsymbol{0} & \boldsymbol{R}_2^{-1} \end{bmatrix} \begin{bmatrix} \boldsymbol{Q}_1^{\mathsf{H}} \\ \boldsymbol{Q}_2^{\mathsf{H}} \end{bmatrix} \\ &= \begin{bmatrix} \boldsymbol{R}_1^{-1}\boldsymbol{Q}_1^{\mathsf{H}} - \boldsymbol{R}_1^{-1}\boldsymbol{S}\boldsymbol{R}_2^{-1}\boldsymbol{Q}_2^{\mathsf{H}} \\ \boldsymbol{R}_2^{-1}\boldsymbol{Q}_2^{\mathsf{H}} \end{bmatrix} . \end{aligned} \tag{B.4}$$

Moreover, since $\boldsymbol{M}_1 = \boldsymbol{Q}_1\boldsymbol{R}_1$, we have

$$\boldsymbol{M}_1^{+} = \boldsymbol{R}_1^{-1}\boldsymbol{Q}_1^{\mathsf{H}} . \tag{B.5}$$

Via (B.4) and (B.5) a relation between the pseudoinverses of $\boldsymbol{M}_\mathrm{a}$ (the entire matrix) and $\boldsymbol{M}_1$ (the left block) is readily established. Using $\boldsymbol{Q}_2^\mathsf{H}\boldsymbol{Q}_1 = \mathbf{0}$ ($[\boldsymbol{Q}_1\ \boldsymbol{Q}_2]$ has orthonormal columns), we have

$$\begin{aligned}\boldsymbol{M}_\mathrm{a}^+(\boldsymbol{M}_1^+)^\mathsf{H} &= \begin{bmatrix} \boldsymbol{R}_1^{-1} & -\boldsymbol{R}_1^{-1}\boldsymbol{S}\boldsymbol{R}_2^{-1} \\ \mathbf{0} & \boldsymbol{R}_2^{-1}\end{bmatrix}\begin{bmatrix}\boldsymbol{Q}_1^\mathsf{H} \\ \boldsymbol{Q}_2^\mathsf{H}\end{bmatrix}(\boldsymbol{R}_1^{-1}\boldsymbol{Q}_1^\mathsf{H})^\mathsf{H} \\ &= \begin{bmatrix} \boldsymbol{R}_1^{-1} & -\boldsymbol{R}_1^{-1}\boldsymbol{S}\boldsymbol{R}_2^{-1} \\ \mathbf{0} & \boldsymbol{R}_2^{-1}\end{bmatrix}\begin{bmatrix}\boldsymbol{R}_1^{-\mathsf{H}} \\ \mathbf{0}\end{bmatrix} \\ &= \begin{bmatrix}\boldsymbol{R}_1^{-1}\boldsymbol{R}_1^{-\mathsf{H}} \\ \mathbf{0}\end{bmatrix}. \end{aligned} \tag{B.6}$$

This means that the last p rows of $\boldsymbol{M}_\mathrm{a}^+$ (the pseudoinverses of the entire matrix) are orthogonal to the rows of $\boldsymbol{M}_1^+$ (the pseudoinverses of the left block).

We are specifically interested in the case $p = 1$; here the partition is given by $\boldsymbol{M}_\mathrm{a} = [\boldsymbol{M}\ \boldsymbol{m}]$, with $\boldsymbol{M} \in \mathbb{C}^{n\times m}$ and $\boldsymbol{m} \in \mathbb{C}^{n\times 1}$ (column vector). The QR decomposition of $\boldsymbol{M}_\mathrm{a}$ is now written as

$$[\boldsymbol{M}\ \boldsymbol{m}] = [\boldsymbol{Q}\ \boldsymbol{q}]\begin{bmatrix}\boldsymbol{R} & \boldsymbol{r} \\ \mathbf{0} & r\end{bmatrix}, \tag{B.7}$$

where $[\boldsymbol{Q}\ \boldsymbol{q}]$ has orthonormal columns, $\boldsymbol{r}$ is a column vector of dimension m and r is a real-valued scalar. The Moore–Penrose inverses (B.5) and (B.4) specialize to

$$\boldsymbol{M}^+ = \boldsymbol{R}^{-1}\boldsymbol{Q}^\mathsf{H}, \tag{B.8}$$

$$\begin{aligned}\boldsymbol{M}_\mathrm{a}^+ &= [\boldsymbol{M}\ \boldsymbol{m}]^+ \\ &= \begin{bmatrix}\boldsymbol{R}^{-1}\boldsymbol{Q}^\mathsf{H} - r^{-1}\boldsymbol{R}^{-1}\boldsymbol{r}\boldsymbol{q}^\mathsf{H} \\ r^{-1}\boldsymbol{q}^\mathsf{H}\end{bmatrix}. \end{aligned} \tag{B.9}$$

The Hermitian of the Moore–Penrose inverse of $\boldsymbol{M}_\mathrm{a}$ and $\boldsymbol{M}$ thus read

$$(\boldsymbol{M}^+)^\mathsf{H} = \boldsymbol{Q}\boldsymbol{R}^{-\mathsf{H}}, \tag{B.10}$$

$$\begin{aligned}(\boldsymbol{M}_\mathrm{a}^+)^\mathsf{H} &= \begin{bmatrix}\boldsymbol{Q}\boldsymbol{R}^{-\mathsf{H}} - r^{-1}\boldsymbol{q}\boldsymbol{r}^\mathsf{H}\boldsymbol{R}^{-\mathsf{H}} & r^{-1}\boldsymbol{q}\end{bmatrix} \\ &\stackrel{\text{def}}{=} [\boldsymbol{X}\ \ \boldsymbol{x}], \end{aligned} \tag{B.11}$$

with obvious definitions of the matrix $\boldsymbol{X} \in \mathbb{C}^{n\times m}$ and the vector $\boldsymbol{x} \in \mathbb{C}^n$.

We are interested in the relation between $(\boldsymbol{M}_{\mathrm{a}}^{+})^{\mathsf{H}}$ and $(\boldsymbol{M}^{+})^{\mathsf{H}}$. To this end, we perform a Gram–Schmidt orthogonalization of the last column in $(\boldsymbol{M}_{\mathrm{a}}^{+})^{\mathsf{H}}$ (which is $\boldsymbol{x} = r^{-1}\boldsymbol{q}$) against all other columns (given by $\boldsymbol{X}$). Obeying $\boldsymbol{q}^{\mathsf{H}}\boldsymbol{q} = 1$ and $\boldsymbol{q}^{\mathsf{H}}\boldsymbol{Q} = \boldsymbol{0}$, this leads to

$$
\begin{aligned}
\boldsymbol{Y} &\overset{\text{def}}{=} \boldsymbol{X} - \boldsymbol{x} \cdot \frac{\boldsymbol{x}^{\mathsf{H}}\boldsymbol{X}}{\boldsymbol{x}^{\mathsf{H}}\boldsymbol{x}} \\
&= \Big(\boldsymbol{I} - \frac{\boldsymbol{x}\boldsymbol{x}^{\mathsf{H}}}{\boldsymbol{x}^{\mathsf{H}}\boldsymbol{x}}\Big)\boldsymbol{X} \\
&= \Big(\boldsymbol{I} - \frac{\boldsymbol{q}\boldsymbol{q}^{\mathsf{H}}}{\boldsymbol{q}^{\mathsf{H}}\boldsymbol{q}}\Big)\boldsymbol{X} \\
&= \Big(\boldsymbol{I} - \boldsymbol{q}\boldsymbol{q}^{\mathsf{H}}\Big)\Big(\boldsymbol{Q}\boldsymbol{R}^{-\mathsf{H}} - r^{-1}\boldsymbol{q}\boldsymbol{r}^{\mathsf{H}}\boldsymbol{R}^{-\mathsf{H}}\Big) \\
&= \boldsymbol{Q}\boldsymbol{R}^{-\mathsf{H}} - \boldsymbol{q}\boldsymbol{q}^{\mathsf{H}}\boldsymbol{Q}\boldsymbol{R}^{-\mathsf{H}} - r^{-1}\boldsymbol{q}\boldsymbol{r}^{\mathsf{H}}\boldsymbol{R}^{-\mathsf{H}} + r^{-1}\boldsymbol{q}\boldsymbol{q}^{\mathsf{H}}\boldsymbol{q}\boldsymbol{r}^{\mathsf{H}}\boldsymbol{R}^{-\mathsf{H}} \\
&= \boldsymbol{Q}\boldsymbol{R}^{-\mathsf{H}} - r^{-1}\boldsymbol{q}\boldsymbol{r}^{\mathsf{H}}\boldsymbol{R}^{-\mathsf{H}} + r^{-1}\boldsymbol{q}\boldsymbol{r}^{\mathsf{H}}\boldsymbol{R}^{-\mathsf{H}} \\
&= \boldsymbol{Q}\boldsymbol{R}^{-\mathsf{H}} \,.
\end{aligned}
\tag{B.12}
$$

Comparing with (B.10), it can be deduced that hat $\boldsymbol{Y} = (\boldsymbol{M}^{+})^{\mathsf{H}}$. Hence, given the inverse of the entire matrix $\boldsymbol{M}_{\mathrm{a}}$, the inverse of the reduced (last columns deleted) matrix can be simply obtained by a Gram–Schmidt orthogonalization step.

Of course, this procedure can be repeated. Starting with the Moore–Penrose inverse of a given matrix, the pseudoinverse of the matrices where the last column is successively deleted can simply be obtained by repeated Gram–Schmidt orthogonalization.

B.2 Classical DFE and the BLAST Approach

In DFE data is successively estimated taking already decoded symbols into account. In contrast to DFE over the temporal dimension, in the MIMO case detection/decoding can be done in an optimized order. Moreover, the combination with channel coding is easily possible: the codewords are arranged over the temporal (horizontal) direction whereas cancellation of interference is done over the users (vertical direction), cf. the H-BLAST approach [46, 47]. As discussed in Chapter 2, the equalization part can hence be optimized as for the uncoded case.

The detection order (sorting of the users) is represented via a *permutation matrix* $\boldsymbol{P}$ of dimension K; it contains a single one in each row and each column and we have the relation $\boldsymbol{P}^{-1} = \boldsymbol{P}^{\mathsf{H}} = \boldsymbol{P}^{\mathsf{T}}$. The MIMO input/output relation (2.12) is then written as

$$\begin{aligned} \boldsymbol{y} = \boldsymbol{H}\boldsymbol{a} + \boldsymbol{n} \;&=\; \boldsymbol{H}\boldsymbol{P}^{-1}\boldsymbol{P}\boldsymbol{a} + \boldsymbol{n} \\ &\stackrel{\text{def}}{=} \boldsymbol{H}\boldsymbol{S}\,\check{\boldsymbol{a}} + \boldsymbol{n}\,, \end{aligned} \tag{B.13}$$

with the matrix $\boldsymbol{S} \stackrel{\text{def}}{=} \boldsymbol{P}^{-1}$ characterizing the reordering (sorting) of the columns of the channel matrix and[1]

$$\check{\boldsymbol{a}} \stackrel{\text{def}}{=} \boldsymbol{P}\boldsymbol{a} \tag{B.14}$$

is the vector of permuted data symbols. The symbols of $\check{\boldsymbol{a}}$ are detected/decoded in the order $l = K, K-1, \ldots, 1$. Without loss of generality, we assume white noise, i.e.,

$$\boldsymbol{\Phi}_{nn} \stackrel{\text{def}}{=} \mathrm{E}\{\boldsymbol{n}\boldsymbol{n}^{\mathsf{H}}\} \;=\; \sigma_n^2 \boldsymbol{I}\;; \tag{B.15}$$

colored noise can be transformed into white noise using a whitening filter, which is incorporated into the channel matrix [31]. The data symbols are also assumed to be uncorrelated,

$$\boldsymbol{\Phi}_{aa} \stackrel{\text{def}}{=} \mathrm{E}\{\boldsymbol{a}\boldsymbol{a}^{\mathsf{H}}\} \;=\; \sigma_a^2 \boldsymbol{I}\,, \tag{B.16}$$

and zero-mean.

[1] In order to distinguish between the action of the permutation matrix $\boldsymbol{P}$ and, later on, that of the integer matrix $\boldsymbol{Z}$, we denote the permuted data vector as $\check{\boldsymbol{a}}$, whereas the vector of integer linear combinations is denoted as $\bar{\boldsymbol{a}}$.

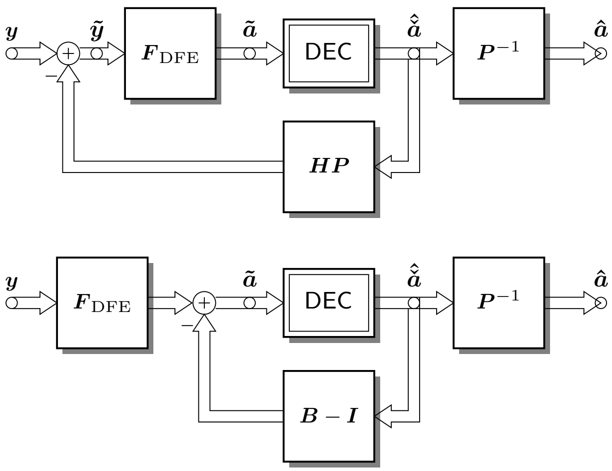

Figure B.1: Receiver structures according to the V-BLAST philosophy (top) and conventional DFE (bottom).

Fig. B.1 shows the receiver structures as used in the derivation of the V-BLAST system [144] (top) and the conventional DFE structure (bottom); both are equivalent [51] and only differ in the point where the interference is canceled (prior to or after the feedforward filter).

The derivations in [46, 144] combine the calculation of the required filter matrices and the detection into a single algorithm. However, when dealing with block-fading channels, the matrices have to be calculated only once per channel realization and then detection is done over the time step using these matrices. We explain the algorithms in the way that they result in the feedforward matrix $\boldsymbol{F}_{\mathrm{DFE}}$, feedback matrix $\boldsymbol{B}$, and the optimal detection order described by the permutation matrix $\boldsymbol{P}$.

Subsequently the detection step (iteration number) is indicated by the superscript $\cdot^{(l)}$; the permuted data vector is partitioned into $\check{\boldsymbol{a}} = \begin{bmatrix} \check{\boldsymbol{a}}_{\mathrm{u}} \\ \check{\boldsymbol{a}}_{\mathrm{d}} \end{bmatrix}$, where the upper part, $\check{\boldsymbol{a}}_{\mathrm{u}}$, corresponds to the still undetected symbols and the lower part, $\check{\boldsymbol{a}}_{\mathrm{d}}$, to the already detected part. The same splitting is done for all other matrices, e.g., $\boldsymbol{H}^{(l)} = \boldsymbol{H}\boldsymbol{S}^{(l)} = [\boldsymbol{H}_{\mathrm{u}}\ \boldsymbol{H}_{\mathrm{d}}]$, where the reordered channel matrix in step l is partitioned such that the left/right columns correspond to the not yet/already decoded symbols, respectively. Moreover, as introduced in Chapter 2, we employ augmented matrices and vectors, e.g., ($\zeta = \sigma_n^2/\sigma_a^2$)

$$\boldsymbol{\mathcal{H}} = \begin{bmatrix} \boldsymbol{H} \\ \sqrt{\zeta}\boldsymbol{I} \end{bmatrix}, \qquad \boldsymbol{\mathcal{y}} = \begin{bmatrix} \boldsymbol{y} \\ \boldsymbol{0} \end{bmatrix} \tag{B.17}$$

are the augmented channel matrix and the augmented receive vector, respectively.

B.2.1 Derivation of BLAST

The V-BLAST strategy for optimal successive detection can be summarized as follows [144]:

- In iteration l, the permuted data symbols $\check{a}_{l+1}, \ldots, \check{a}_K$, i.e., the elements of the vector $\check{\boldsymbol{a}}_\mathrm{d}$, are already detected; their influence on the received signal is canceled.
- The linear estimators for the remaining symbols $\check{a}_1, \ldots, \check{a}_l$, i.e., the elements of the vector $\check{\boldsymbol{a}}_\mathrm{u}$, and the corresponding estimation variances are calculated.
- Only the symbol which can be detected most reliably (having the smallest estimation variance) is actually detected in iteration l.
- The estimation vector for the best symbol gives the l^{th} row of the feedforward matrix $\boldsymbol{F}_\mathrm{DFE}$; the channel matrix is reordered accordingly (sorting $\boldsymbol{S}$).
- The procedure is repeated from $l = K$ through $l = 1$.

We now take a closer look at the calculated MMSE estimators and the induced sorting. We do this using the principle of mathematical induction.

Base Case

The optimal linear MMSE estimator in the initial step ($l = K$) is the same as for linear equalization (cf. (2.16), (2.18)). The MMSE estimate is given by

$$\tilde{\boldsymbol{a}}_\mathrm{u}^{(K)} = (\boldsymbol{H}^\mathsf{H}\boldsymbol{H} + \zeta\boldsymbol{I})^{-1}\boldsymbol{H}^\mathsf{H}\boldsymbol{y} \,,$$

$$
\begin{aligned}
&= \left([\boldsymbol{H}^{\mathsf{H}} \; \sqrt{\zeta}\boldsymbol{I}] \begin{bmatrix} \boldsymbol{H} \\ \sqrt{\zeta}\boldsymbol{I} \end{bmatrix} \right)^{-1} [\boldsymbol{H}^{\mathsf{H}} \; \sqrt{\zeta}\boldsymbol{I}] \begin{bmatrix} \boldsymbol{y} \\ \boldsymbol{0} \end{bmatrix} \\
&= \boldsymbol{\mathcal{H}}^{+}\boldsymbol{y} \; ,
\end{aligned}
$$

i.e., the feedforward filter $\boldsymbol{\mathcal{F}}_{\mathrm{u}}^{(K)} = \boldsymbol{\mathcal{H}}^{+}$ is given by the pseudoinverse of the augmented channel matrix. The mean-squared error (MSE), i.e., the variance of the estimation error $\tilde{\boldsymbol{n}} \stackrel{\text{def}}{=} \check{\boldsymbol{a}}_{\mathrm{u}}^{(K)} - \boldsymbol{a}$, is given by the main-diagonal elements of [105, 31]

$$
\begin{aligned}
\boldsymbol{\Phi}_{\tilde{n}\tilde{n}} &\stackrel{\text{def}}{=} \mathrm{E}\{\tilde{\boldsymbol{n}}\tilde{\boldsymbol{n}}^{\mathsf{H}}\} \\
&= \sigma_n^2 \, (\boldsymbol{\mathcal{H}}^{\mathsf{H}}\boldsymbol{\mathcal{H}})^{-1} \; . \qquad \text{(B.18)}
\end{aligned}
$$

The smallest main-diagonal element of $\boldsymbol{\Phi}_{\tilde{n}\tilde{n}}$ is identified; the index $k_{\mathrm{b}}^{(K)}$ gives the user to be detected first (the user with the smallest noise enhancement). The $(k_{\mathrm{b}}^{(K)})^{\mathrm{th}}$ row of $\boldsymbol{\mathcal{F}}_{\mathrm{u}}^{(K)}$ gives the last, i.e., K^{th}, row of the final feedforward matrix $\boldsymbol{\mathcal{F}}$. The new channel matrix $\boldsymbol{\mathcal{H}}^{(K-1)}$ is obtained from $\boldsymbol{\mathcal{H}}$ by moving the $(k_{\mathrm{b}}^{(K)})^{\mathrm{th}}$ column to the end (i.e., rightmost position). This reordering is recorded in the permutation matrix; the $(k_{\mathrm{b}}^{(K)})^{\mathrm{th}}$ column of $\boldsymbol{S}^{(K)} = \boldsymbol{I}$ is moved to the end.

Induction Step

In iteration l the current augmented channel matrix $\boldsymbol{\mathcal{H}}^{(l)}$ is sorted such that the columns corresponding to the already decoded users form the right part and the columns corresponding to the not yet decoded users form the left part, i.e.,[2]

$$
\boldsymbol{\mathcal{H}}^{(l)} = \boldsymbol{\mathcal{H}}\boldsymbol{S}^{(l)} = [\boldsymbol{\mathcal{H}}_{\mathrm{u}} \; \boldsymbol{\mathcal{H}}_{\mathrm{d}}] = \left[\begin{bmatrix} \boldsymbol{H}_{\mathrm{u}} \\ \sqrt{\zeta}\boldsymbol{S}_{\mathrm{u}} \end{bmatrix} \begin{bmatrix} \boldsymbol{H}_{\mathrm{d}} \\ \sqrt{\zeta}\boldsymbol{S}_{\mathrm{d}} \end{bmatrix} \right] . \qquad \text{(B.19)}
$$

The contributions of the already detected users are canceled, leading to

$$
\tilde{\boldsymbol{y}}^{(l)} \stackrel{\text{def}}{=} \boldsymbol{y} - \boldsymbol{H}_{\mathrm{d}}\check{\boldsymbol{a}}_{\mathrm{d}} \; . \qquad \text{(B.20)}
$$

Here we define the augmented receive vector where interference is canceled as

$$
\tilde{\boldsymbol{\mathcal{y}}}^{(l)} \stackrel{\text{def}}{=} \boldsymbol{\mathcal{y}} - \boldsymbol{\mathcal{H}}_{\mathrm{d}}\check{\boldsymbol{a}}_{\mathrm{d}} = \begin{bmatrix} \tilde{\boldsymbol{y}}^{(l)} \\ \sqrt{\zeta}\boldsymbol{S}_{\mathrm{d}}\check{\boldsymbol{a}}_{\mathrm{d}} \end{bmatrix} . \qquad \text{(B.21)}
$$

[2] For readability the superscript $\cdot^{(l)}$ for the iteration is omitted for the partial matrices and the partial vectors.

Then, the MMSE estimate for the remaining users is calculated. Since $\boldsymbol{S}_{\mathrm{u}}^{\mathsf{H}}\boldsymbol{S}_{\mathrm{u}} = \boldsymbol{I}$ and $\boldsymbol{S}_{\mathrm{u}}^{\mathsf{H}}\boldsymbol{S}_{\mathrm{d}} = \boldsymbol{0}$ (parts of a permutation matrix), the MMSE estimate reads

$$\begin{aligned}
\tilde{\boldsymbol{a}}_{\mathrm{u}}^{(l)} &= (\boldsymbol{H}_{\mathrm{u}}^{\mathsf{H}}\boldsymbol{H}_{\mathrm{u}} + \zeta\boldsymbol{I})^{-1}\boldsymbol{H}_{\mathrm{u}}^{\mathsf{H}}\,\tilde{\boldsymbol{y}}^{(l)} \\
&= \left([\boldsymbol{H}_{\mathrm{u}}^{\mathsf{H}}\ \sqrt{\zeta}\boldsymbol{S}_{\mathrm{u}}^{\mathsf{H}}]\begin{bmatrix}\boldsymbol{H}_{\mathrm{u}} \\ \sqrt{\zeta}\boldsymbol{S}_{\mathrm{u}}\end{bmatrix}\right)^{-1}[\boldsymbol{H}_{\mathrm{u}}^{\mathsf{H}}\ \sqrt{\zeta}\boldsymbol{S}_{\mathrm{u}}^{\mathsf{H}}]\begin{bmatrix}\tilde{\boldsymbol{y}}^{(l)} \\ \sqrt{\zeta}\boldsymbol{S}_{\mathrm{d}}\check{\boldsymbol{a}}_{\mathrm{d}}\end{bmatrix} \\
&= \boldsymbol{\mathcal{H}}_{\mathrm{u}}^{+}\tilde{\underline{\boldsymbol{y}}}^{(l)}\,,
\end{aligned} \tag{B.22}$$

hence the receive matrix $\boldsymbol{\mathcal{F}}_{\mathrm{u}}^{(l)} = \boldsymbol{\mathcal{H}}_{\mathrm{u}}^{+}$ in step l is the pseudoinverse of the left part of the sorted augmented channel matrix. The MSE is given by the main-diagonal elements of the error covariance matrix

$$\boldsymbol{\Phi}_{\tilde{n}\tilde{n}} = \sigma_n^2\,(\boldsymbol{\mathcal{H}}_{\mathrm{u}}^{\mathsf{H}}\boldsymbol{\mathcal{H}}_{\mathrm{u}})^{-1} \tag{B.23}$$

which can be written as

$$\begin{aligned}
\boldsymbol{\Phi}_{\tilde{n}\tilde{n}} &= \sigma_n^2\,(\boldsymbol{\mathcal{H}}_{\mathrm{u}}^{\mathsf{H}}\boldsymbol{\mathcal{H}}_{\mathrm{u}})^{-1}\boldsymbol{\mathcal{H}}_{\mathrm{u}}^{\mathsf{H}}\cdot\boldsymbol{\mathcal{H}}_{\mathrm{u}}(\boldsymbol{\mathcal{H}}_{\mathrm{u}}^{\mathsf{H}}\boldsymbol{\mathcal{H}}_{\mathrm{u}})^{-1} \\
&= \sigma_n^2\,\boldsymbol{\mathcal{H}}_{\mathrm{u}}^{+}(\boldsymbol{\mathcal{H}}_{\mathrm{u}}^{+})^{\mathsf{H}} \\
&= \sigma_n^2\,(\boldsymbol{\mathcal{F}}_{\mathrm{u}}^{(l)})^{\mathsf{H}}\boldsymbol{\mathcal{F}}_{\mathrm{u}}^{(l)}\,.
\end{aligned} \tag{B.24}$$

Since the main-diagonal elements of the last product are equal to the row norms of $\boldsymbol{\mathcal{F}}^{(l)}$, the noise enhancement (or, when multiplied with σ_n^2, the mean-squared error) is given by the row norms of the augmented receive matrix.

Among the remaining users, the user (index $k_{\mathrm{b}}^{(l)}$) with the currently lowest noise enhancement is decoded at the present step l. The $(k_{\mathrm{b}}^{(l)})^{\mathrm{th}}$ row of $\boldsymbol{\mathcal{F}}_{\mathrm{u}}^{(l)}$ gives the l^{th} row of $\boldsymbol{\mathcal{F}}$.

Due to the specific calculation of $\boldsymbol{\mathcal{F}}_{\mathrm{u}}^{(l)}$ we have

$$\begin{aligned}
\boldsymbol{\mathcal{F}}_{\mathrm{u}}^{(l)}\boldsymbol{\mathcal{H}}^{(l)} &= (\boldsymbol{\mathcal{H}}_{\mathrm{u}})^{+}\,[\boldsymbol{\mathcal{H}}_{\mathrm{u}}\ \boldsymbol{\mathcal{H}}_{\mathrm{d}}] \\
&= [\boldsymbol{I} \quad \boldsymbol{X}]
\end{aligned} \tag{B.25}$$

where $\boldsymbol{X}$ remains unspecified for the moment. Moreover, since equalization is only done w.r.t. the not yet detected users we can write

$$\boldsymbol{\mathcal{F}}_{\mathrm{d}}^{(l)}\boldsymbol{\mathcal{H}}^{(l)} = [\boldsymbol{0}\ \ \boldsymbol{R}_{\mathrm{d}}]\,, \tag{B.26}$$

where $\boldsymbol{R}_{\mathrm{d}}$ is an upper triangular matrix with unit main diagonal. Hence, in total

$$\begin{bmatrix} \boldsymbol{\mathcal{F}}_{\mathrm{u}}^{(l)} \\ \boldsymbol{\mathcal{F}}_{\mathrm{d}}^{(l)} \end{bmatrix} \boldsymbol{\mathcal{H}} \boldsymbol{S}^{(l)} = \begin{bmatrix} \boldsymbol{I} & \boldsymbol{X} \\ \boldsymbol{0} & \boldsymbol{R}_{\mathrm{d}} \end{bmatrix} . \tag{B.27}$$

Note that $\boldsymbol{\mathcal{F}}_{\mathrm{u}}^{(l)}$ is the pseudoinverse of the left part of the matrix $\boldsymbol{\mathcal{H}}^{(l)}$ and the rows of $\boldsymbol{\mathcal{F}}_{\mathrm{d}}^{(l)}$ are rows of the pseudoinverse of the entire matrix $\boldsymbol{\mathcal{H}}^{(l)}$. Hence, according to (B.6), the rows of $\boldsymbol{\mathcal{F}}_{\mathrm{u}}^{(l)}$ are orthogonal to that of $\boldsymbol{\mathcal{F}}_{\mathrm{d}}^{(l)}$. In the final step, we arrive at

$$\boldsymbol{\mathcal{F}} \boldsymbol{\mathcal{H}} \boldsymbol{S} = \boldsymbol{R} , \tag{B.28}$$

where $\boldsymbol{\mathcal{F}}$ has orthogonal rows (white noise remains white while filtering with the DFE feedforward filter) and $\boldsymbol{R}$ is an upper triangular matrix.

Thus, over the iterations the V-BLAST algorithm induces a (sorted) QR decomposition of the channel matrix. Defining $\boldsymbol{\mathcal{O}} = \boldsymbol{\mathcal{F}}^{+}$ and obeying $\boldsymbol{S} = \boldsymbol{P}^{-1} = \boldsymbol{P}^{\mathsf{H}}$, we have

$$\boldsymbol{\mathcal{H}} \boldsymbol{P}^{\mathsf{H}} = \boldsymbol{\mathcal{O}} \boldsymbol{R} , \tag{B.29}$$

Moving the subtraction point from the input of the feedforward filter to its output, we moreover see that the feedback matrix in the DFE structure is given by $\boldsymbol{B} = \boldsymbol{R}$ as

$$\begin{aligned} \tilde{\boldsymbol{a}} &= \boldsymbol{\mathcal{F}} \tilde{\boldsymbol{y}} \\ &= \boldsymbol{\mathcal{F}} (\boldsymbol{y} - \boldsymbol{\mathcal{H}} \boldsymbol{S} \check{\boldsymbol{a}}) \\ &= \boldsymbol{\mathcal{F}} \boldsymbol{y} - \boldsymbol{R} \check{\boldsymbol{a}} . \end{aligned} \tag{B.30}$$

The notation $\boldsymbol{B} - \boldsymbol{I}$ instead of $\boldsymbol{B}$ in the block diagrams indicates that the cancellation of symbol l from its own data stream l is neither required nor can it be carried out in a causal way; hence the unit-gain main diagonal elements of $\boldsymbol{B} = \boldsymbol{R}$ are eliminated for the feedback calculation.

B.2.2 Dual-Lattice Approach

The V-BLAST procedure results in the optimal (w.r.t. worst-link performance [144]) detection order and corresponding feedforward and feedback matrices. However, it requires a large effort as repeatedly pseudoinverses have to be calculated. Hence, low-complexity variants which also give the optimum solution, have been proposed. The most prominent are the "square root" algorithm in [55], the recursive rank-one update algorithm in [5], and the "dual-lattice" approach in [82]. Although not identical, they share the philosophy of avoiding the repeated calculations of pseudoinverses via low-complexity updates on an initial solution.

In this subsection, in view of the subsequent generalization to LRA schemes, we re-derive the dual-lattice approach and prove that it leads to the same results as the V-BLAST procedure.

In the dual-lattice approach, the Hermitian of the pseudoinverse of the augmented channel matrix is calculated

$$(\boldsymbol{\mathcal{H}}^{+})^{\mathsf{H}} = ((\boldsymbol{\mathcal{H}}^{\mathsf{H}}\boldsymbol{\mathcal{H}})^{-1}\boldsymbol{\mathcal{H}}^{\mathsf{H}})^{\mathsf{H}} = \boldsymbol{\mathcal{H}}(\boldsymbol{\mathcal{H}}^{\mathsf{H}}\boldsymbol{\mathcal{H}})^{-1} \tag{B.31}$$

and a sorted (with pivoting) Gram–Schmidt procedure (from $l = K$ to $l = 1$) is carried out leading to (cf. [38])

$$(\boldsymbol{\mathcal{H}}^{+})^{\mathsf{H}}\boldsymbol{S} = \boldsymbol{\mathcal{Q}}\boldsymbol{L}\,, \tag{B.32}$$

where $\boldsymbol{\mathcal{Q}}$ has orthogonal columns, $\boldsymbol{L}$ is *lower* triangular with unit main-diagonal, and $\boldsymbol{S}$ is a permutation matrix. Since operations are carried out on $(\boldsymbol{\mathcal{H}}^{+})^{\mathsf{H}}$ and this matrix is the generator matrix $\boldsymbol{G}^{\perp}$ of the dual lattice to that spanned by $\boldsymbol{\mathcal{H}}$ (cf. Sec. A.1), this procedure is usually denoted as *"dual-lattice approach"*.

We now show by mathematical induction that these matrices are related to those of the V-BLAST procedure as $\boldsymbol{\mathcal{Q}}^{\mathsf{H}} = \boldsymbol{\mathcal{F}}$ and $\boldsymbol{L}^{-\mathsf{H}} = \boldsymbol{R}$ and that the same permutation matrix $\boldsymbol{S}$ is obtained.

Base Case

For $l = K$, the initialization is given by

$$\boldsymbol{\mathcal{Q}}^{(K)} = (\boldsymbol{\mathcal{H}}^{+})^{\mathsf{H}} \qquad \boldsymbol{L}^{(K)} = \boldsymbol{I}\,, \tag{B.33}$$

and pivoting is done according to the column of $\boldsymbol{\mathcal{Q}}^{(K)}$ with the *least* norm. The column norms are the main-diagonal elements of

$$\begin{aligned}(\boldsymbol{\mathcal{Q}}^{(K)})^{\mathsf{H}}\boldsymbol{\mathcal{Q}}^{(K)} &= \boldsymbol{\mathcal{H}}^{+}(\boldsymbol{\mathcal{H}}^{+})^{\mathsf{H}} \\ &= (\boldsymbol{\mathcal{H}}^{\mathsf{H}}\boldsymbol{\mathcal{H}})^{-1}\boldsymbol{\mathcal{H}}^{\mathsf{H}} \cdot \boldsymbol{\mathcal{H}}(\boldsymbol{\mathcal{H}}^{\mathsf{H}}\boldsymbol{\mathcal{H}})^{-1} \\ &= (\boldsymbol{\mathcal{H}}^{\mathsf{H}}\boldsymbol{\mathcal{H}})^{-1} . \end{aligned} \tag{B.34}$$

Hence we can conclude that for the base case the V-BLAST approach and the dual-lattice approach use the same matrices, i.e., $(\boldsymbol{\mathcal{Q}}^{(K)})^{\mathsf{H}} = \boldsymbol{\mathcal{F}}_{\mathrm{u}}^{(K)}$, and find the same minimum as criteria (B.18) and (B.34) are identical. Hence, the last row in $\boldsymbol{\mathcal{F}}$ will be identical to the rightmost column in $\boldsymbol{\mathcal{Q}}$ (which is never changed during the GSO process) and the same permutation matrices are present.

Induction Step

In iteration l, since a GSO is performed, we have

$$\begin{aligned}(\boldsymbol{\mathcal{H}}^{+})^{\mathsf{H}}\boldsymbol{S}^{(l)} &= \boldsymbol{\mathcal{Q}}^{(l)}\boldsymbol{L}^{(l)} \\ &= [\boldsymbol{\mathcal{Q}}_{\mathrm{u}}\ \boldsymbol{\mathcal{Q}}_{\mathrm{d}}]\begin{bmatrix}\boldsymbol{I} & \boldsymbol{0} \\ \boldsymbol{X} & \boldsymbol{L}_{\mathrm{d}}\end{bmatrix} , \end{aligned} \tag{B.35}$$

where the columns of $\boldsymbol{\mathcal{Q}}_{\mathrm{d}}$ are orthogonal to each other, $\boldsymbol{L}_{\mathrm{d}}$ is lower triangular with unit main diagonal, and $\boldsymbol{X}$ is not specified for the moment.

Assume that $\boldsymbol{\mathcal{F}}_{\mathrm{d}} = \boldsymbol{\mathcal{Q}}_{\mathrm{d}}^{\mathsf{H}}$ and the same sorting $\boldsymbol{S}^{(l)}$ has been found up to now in both approaches. Then the sorted augmented channel matrix $\boldsymbol{\mathcal{H}}^{(l)} = \boldsymbol{\mathcal{H}}\boldsymbol{S}^{(l)} = [\boldsymbol{\mathcal{H}}_{\mathrm{u}}\ \ \boldsymbol{\mathcal{H}}_{\mathrm{d}}]$ is the same as in V-BLAST. Moreover, since in V-BLAST the next estimation matrix is $\boldsymbol{\mathcal{F}}_{\mathrm{u}} = \boldsymbol{\mathcal{H}}_{\mathrm{u}}^{+}$ and, as shown in Sec. B.1, a Gram–Schmidt orthogonalization on $\boldsymbol{\mathcal{Q}}$ results in $\boldsymbol{\mathcal{Q}}_{\mathrm{u}} = (\boldsymbol{\mathcal{H}}_{\mathrm{u}}^{+})^{\mathsf{H}}$, we conclude that $\boldsymbol{\mathcal{F}}_{\mathrm{u}} = \boldsymbol{\mathcal{Q}}_{\mathrm{u}}^{\mathsf{H}}$.

Since the column of $\boldsymbol{\mathcal{Q}}_{\mathrm{u}}$ with the least norm is selected next and this is identical to choosing the row in $\boldsymbol{\mathcal{F}}_{\mathrm{u}}$ with the least norm (cf. (B.24), in both approaches the next user to be decoded is the same. Hence, the same next permutation matrix is obtained and the same row is appended to $\boldsymbol{\mathcal{Q}}_{\mathrm{d}}^{\mathsf{H}}$ and $\boldsymbol{\mathcal{F}}_{\mathrm{d}}$, respectively.

Consequently, due to induction, both approaches lead to the same sorting matrix $\boldsymbol{S}$ and feedforward matrix $\boldsymbol{\mathcal{F}} = \boldsymbol{\mathcal{Q}}^{\mathsf{H}}$, respectively, and also to the same feedback matrix $\boldsymbol{B} = \boldsymbol{L}^{-\mathsf{H}}$, which can be seen when solving (B.32) for $\boldsymbol{L}^{-\mathsf{H}}$ as

$$\begin{aligned}
\boldsymbol{L}^{-\mathsf{H}} &\overset{(\text{B.32})}{=} \left(\boldsymbol{\mathcal{Q}}^{+}(\boldsymbol{\mathcal{H}}^{+})^{\mathsf{H}}\boldsymbol{S}\right)^{-\mathsf{H}} \\
&\overset{\boldsymbol{S}^{-1}=\boldsymbol{S}^{\mathsf{H}}}{=} \left(\boldsymbol{\mathcal{H}}^{+}(\boldsymbol{\mathcal{Q}}^{+})^{\mathsf{H}}\right)^{+}\boldsymbol{S} \\
&= \boldsymbol{\mathcal{Q}}^{\mathsf{H}}\boldsymbol{\mathcal{H}}\boldsymbol{S} \\
&\overset{(\text{B.29})}{=} \boldsymbol{B}\,.
\end{aligned} \tag{B.36}$$

In summary, the optimal equalization matrices for conventional DFE obeying the BLAST approach can be efficiently calculated by a conventional Gram–Schmidt orthogonalization procedure with suited pivoting, cf. [38]. Thereby, the Hermitian pseudoinverse of the augmented channel matrix, i.e., $(\boldsymbol{\mathcal{H}}^{+})^{\mathsf{H}}$, can also be calculated applying a Gram–Schmidt procedure to obtain the QR decomposition (B.2).

B.3 LRA DFE and Adapted Lattice Reduction Algorithm

We now turn to LRA DFE and the question how to calculate the feed-forward matrix $\boldsymbol{F}$, feedback matrix $\boldsymbol{B}$, and integer matrix $\boldsymbol{Z}$ for optimal performance. As LRA DFE (cf. Chapter 3) can be seen as a generalization of conventional DFE where the permutation matrix $\boldsymbol{P}$ is replaced by the integer matrix $\boldsymbol{Z}$, the derivations, in some sense, are generalizations of that given above. As before, we start with the main principles from estimation theory and then show how to efficiently solve the resulting factorization task.

B.3.1 Derivation of "LRA-BLAST"

For the subsequent derivations, Fig. B.1 is still valid if $\boldsymbol{P}$ is replaced by the more general integer matrix $\boldsymbol{Z}$, cf. also Fig. 5.1. As in (3.1) we define the reduced channel matrix $\boldsymbol{W}$ and its augmented version by $\boldsymbol{\mathcal{W}}$ by

$$\boldsymbol{W} \stackrel{\text{def}}{=} \boldsymbol{H}\,\boldsymbol{Z}^{-1} \tag{B.37}$$

$$\boldsymbol{\mathcal{W}} \stackrel{\text{def}}{=} \boldsymbol{\mathcal{H}}\boldsymbol{Z}^{-1} = \begin{bmatrix} \boldsymbol{W} \\ \sqrt{\zeta}\boldsymbol{Z}^{-1} \end{bmatrix} = \begin{bmatrix} \boldsymbol{W} \\ \sqrt{\zeta}\boldsymbol{V} \end{bmatrix}, \tag{B.38}$$

with

$$\boldsymbol{V} \stackrel{\text{def}}{=} \boldsymbol{Z}^{-1}\,. \tag{B.39}$$

The Hermitian of the integer matrix is written as column-wise partitioned, i.e., $\boldsymbol{Z}^{\mathsf{H}} = [\boldsymbol{z}_1, \ldots, \boldsymbol{z}_K]$.

As already observed in Chapter 3, the integer linear combinations $\bar{\boldsymbol{a}}$ are *correlated*; the correlation matrix is given by

$$\boldsymbol{\Phi}_{\bar{a}\bar{a}} \stackrel{\text{def}}{=} \mathrm{E}\{\bar{\boldsymbol{a}}\bar{\boldsymbol{a}}^{\mathsf{H}}\} = \sigma_a^2 \boldsymbol{Z}\boldsymbol{Z}^{\mathsf{H}} = \sigma_a^2 \boldsymbol{V}^{-1}\boldsymbol{V}^{-\mathsf{H}}\,; \tag{B.40}$$

this is one of the main differences to conventional DFE.

We now take a detailed look on the calculation of the optimal MMSE estimators and the respective integer matrix. We do this again using the principle of mathematical induction.

Base Case

The optimal linear MMSE estimator in the initial step is the same as in LRA linear equalization (cf. (3.3) and (3.6)). Assume for the moment that the integer matrix $\boldsymbol{Z}$ is fixed and hence the correlations are known. In case of white noise, i.e., $\boldsymbol{\Phi}_{nn} = \sigma_n^2 \boldsymbol{I}$, the MMSE estimate is then given by [105]

$$
\begin{aligned}
\check{\boldsymbol{a}}_{\mathrm{u}}^{(K)} &= \left(\boldsymbol{W}^{\mathsf{H}} \boldsymbol{\Phi}_{nn}^{-1} \boldsymbol{W} + \boldsymbol{\Phi}_{\bar{a}\bar{a}}\right)^{-1} \boldsymbol{W}^{\mathsf{H}} \boldsymbol{\Phi}_{nn}^{-1} \boldsymbol{y} \\
&= \left(\boldsymbol{W}^{\mathsf{H}} \boldsymbol{W} + \zeta \boldsymbol{Z}^{-\mathsf{H}} \boldsymbol{Z}^{-1}\right)^{-1} \boldsymbol{W}^{\mathsf{H}} \boldsymbol{y} \\
&= \left(\boldsymbol{\mathcal{W}}^{\mathsf{H}} \boldsymbol{\mathcal{W}}\right)^{-1} \boldsymbol{\mathcal{W}}^{\mathsf{H}} \boldsymbol{\mathcal{y}} \\
&= \boldsymbol{Z} \left(\boldsymbol{\mathcal{H}}^{\mathsf{H}} \boldsymbol{\mathcal{H}}\right)^{-1} \boldsymbol{\mathcal{H}}^{\mathsf{H}} \boldsymbol{\mathcal{y}} \\
&= \boldsymbol{Z} \boldsymbol{\mathcal{H}}^{+} \boldsymbol{\mathcal{y}} \,,
\end{aligned}
\tag{B.41}
$$

where again the augmented receive vector from (B.17) has been used. The MMSE estimator is hence equal to $\boldsymbol{\mathcal{F}}_{\mathrm{u}}^{(K)} = \boldsymbol{Z}\boldsymbol{\mathcal{H}}^{+}$. The MSE, i.e., the variance of the estimation error $\tilde{\boldsymbol{n}} \overset{\text{def}}{=} \check{\boldsymbol{a}}_{\mathrm{u}}^{(K)} - \bar{\boldsymbol{a}}$, is given by the main-diagonal elements of (cf. (3.6))

$$
\begin{aligned}
\boldsymbol{\Phi}_{\tilde{n}\tilde{n}} &= \sigma_n^2 \left(\boldsymbol{\mathcal{W}}^{\mathsf{H}} \boldsymbol{\mathcal{W}}\right)^{-1} \\
&= \sigma_n^2 \, \boldsymbol{Z} \left(\boldsymbol{\mathcal{H}}^{\mathsf{H}} \boldsymbol{\mathcal{H}}\right)^{-1} \boldsymbol{Z}^{\mathsf{H}} \,.
\end{aligned}
\tag{B.42}
$$

In contrast to LRA linear equalization, in the current step we are not interested in the entire matrix $\boldsymbol{Z}$, but in an integer vector, as in LRA DFE only a single data stream is detected in each iteration. Since detection is done in sequence $l = K$ through $l = 1$, in the base case we may choose $\boldsymbol{z}_K$, i.e., build the best integer linear combination out of the K parallel data streams, such that[3]

$$
\begin{aligned}
\boldsymbol{z}_K^{\mathsf{H}} \left(\boldsymbol{\mathcal{H}}^{\mathsf{H}} \boldsymbol{\mathcal{H}}\right)^{-1} \boldsymbol{z}_K &= \boldsymbol{z}_K^{\mathsf{H}} \boldsymbol{\mathcal{H}}^{+} (\boldsymbol{\mathcal{H}}^{+})^{\mathsf{H}} \boldsymbol{z}_K \\
&= ||(\boldsymbol{\mathcal{H}}^{+})^{\mathsf{H}} \boldsymbol{z}_K||^2
\end{aligned}
\tag{B.43}
$$

is minimized over the choice of the integer vector $\boldsymbol{z}_K$. This is a *shortest vector problem* (cf. Appendix A).

[3] Please note that $\left(\boldsymbol{\mathcal{H}}^{\mathsf{H}} \boldsymbol{\mathcal{H}}\right)^{-1} = \left(\boldsymbol{\mathcal{H}}^{\mathsf{H}} \boldsymbol{\mathcal{H}}\right)^{-1} \boldsymbol{\mathcal{H}}^{\mathsf{H}} \boldsymbol{\mathcal{H}} \left(\boldsymbol{\mathcal{H}}^{\mathsf{H}} \boldsymbol{\mathcal{H}}\right)^{-1} = \boldsymbol{\mathcal{H}}^{+} (\boldsymbol{\mathcal{H}}^{+})^{\mathsf{H}}$.

Having a solution, $\boldsymbol{z}_K^{\mathsf{H}}\boldsymbol{\mathcal{H}}^+$ gives the last row of the final feedforward matrix $\boldsymbol{\mathcal{F}}$ and $\boldsymbol{z}_K$ is the last column of the Hermitian of the final integer matrix. Both items are never changed in the subsequent steps. However, as will be discussed later in detail, we might have some constraint on the integer matrix $\boldsymbol{Z}$. Starting with $\boldsymbol{Z} = \boldsymbol{I}$ and updating only the last columns might destroy this constraint. Hence, whenever a new column is forced in $\boldsymbol{Z}^{\mathsf{H}}$ (row in $\boldsymbol{Z}$) the not yet fixed columns ($\boldsymbol{z}_1$ through $\boldsymbol{z}_{l-1}$ in iteration l) have to be updated adequately. The same holds for the inverse of $\boldsymbol{Z}$, i.e., $\boldsymbol{V}$. Subsequently, we will discuss how this is done in detail.

Induction Step

In iteration l, the linear combinations $\bar{a}_{l+1}, \ldots, \bar{a}_K$ have already been detected; the symbols $\bar{a}_1, \ldots, \bar{a}_l$ still have to be determined with the aid of the already available knowledge. To this end, we partition the matrices according to the part corresponding to the already detected/decoded linear combinations (right part "d") and that corresponding to the not yet detected/decoded linear combinations (left part "u"); in particular we have

$$\boldsymbol{Z}^{\mathsf{H}} = [\,\boldsymbol{Z}_{\mathrm{u}}\,\boldsymbol{Z}_{\mathrm{d}}\,]\,, \qquad \boldsymbol{V} = [\,\boldsymbol{V}_{\mathrm{u}}\,\boldsymbol{V}_{\mathrm{d}}\,]\,, \qquad \boldsymbol{W} = [\,\boldsymbol{W}_{\mathrm{u}}\,\boldsymbol{W}_{\mathrm{d}}\,] \tag{B.44}$$

and

$$\boldsymbol{\mathcal{W}}^{(l)} = \boldsymbol{\mathcal{H}}(\boldsymbol{Z}^{(l)})^{-1} = [\boldsymbol{\mathcal{W}}_{\mathrm{u}}\,\boldsymbol{\mathcal{W}}_{\mathrm{d}}] = \left[\begin{bmatrix}\boldsymbol{W}_{\mathrm{u}}\\ \sqrt{\zeta}\boldsymbol{V}_{\mathrm{u}}\end{bmatrix}\begin{bmatrix}\boldsymbol{W}_{\mathrm{d}}\\ \sqrt{\zeta}\boldsymbol{V}_{\mathrm{d}}\end{bmatrix}\right]. \tag{B.45}$$

The respective partitioning also is done for the vector of integer linear combinations, i.e., $\bar{\boldsymbol{a}} = \begin{bmatrix}\bar{\boldsymbol{a}}_{\mathrm{u}}\\ \bar{\boldsymbol{a}}_{\mathrm{d}}\end{bmatrix}$.

As already emphasized, in LRA DFE correlated data is successively estimated. Assume for the moment that the integer matrix $\boldsymbol{Z}$ is fixed and hence the correlations[4] (covariance matrix $\boldsymbol{\Phi}_{\bar{a}\bar{a}}$, cf. (B.40)) of the data are known. Having the observation $\boldsymbol{y} = \boldsymbol{W}\bar{\boldsymbol{a}} + \boldsymbol{n}$, the optimal procedure is as follows:

A) As in conventional DFE, the influence of the already detected symbols is canceled from the receive vector $\boldsymbol{y}$. This is done by remod-

[4] We assume zero-mean data; offsets are eliminated.

ulating the vector $\hat{\bar{\boldsymbol{a}}}_{\mathrm{d}}$ of decisions via $\boldsymbol{W}_{\mathrm{d}}$ and calculating

$$\tilde{\boldsymbol{y}}^{(l)} \overset{\mathrm{def}}{=} \boldsymbol{y} - \boldsymbol{W}_{\mathrm{d}}\hat{\bar{\boldsymbol{a}}}_{\mathrm{d}} \,. \tag{B.46}$$

B) The symbols of the unknown part $\bar{\boldsymbol{a}}_{\mathrm{u}} = [\bar{a}_1, \ \ldots, \ \bar{a}_l]^{\mathsf{T}}$ are correlated with the symbols of the known part $\bar{\boldsymbol{a}}_{\mathrm{d}} = [\bar{a}_{l+1}, \ \ldots, \ \bar{a}_K]^{\mathsf{T}}$. This p-priori knowledge has to be taken into account in the estimation process, expressed as a known mean $\boldsymbol{\mu}_{\mathrm{u|d}}$ of $\bar{\boldsymbol{a}}_{\mathrm{u}}$. This mean and the covariance matrix of the remaining error $\boldsymbol{e}_{\bar{a}_{\mathrm{d}}} = \bar{\boldsymbol{a}}_{\mathrm{d}} - \boldsymbol{\mu}_{\mathrm{u|d}}$ are obtained as follows.

The correlation matrix (B.40) may be decomposed according to

$$\boldsymbol{\Phi}_{\bar{a}\bar{a}} = \begin{bmatrix} \boldsymbol{\Phi}_{\mathrm{uu}} & \boldsymbol{\Phi}_{\mathrm{ud}} \\ \boldsymbol{\Phi}_{\mathrm{du}} & \boldsymbol{\Phi}_{\mathrm{dd}} \end{bmatrix} . \tag{B.47}$$

On the one hand, the inverse is given by [63] (the elements "$*$" are irrelevant here)

$$\boldsymbol{\Phi}_{\bar{a}\bar{a}}^{-1} = \begin{bmatrix} \boldsymbol{\Phi}_{\mathrm{uu|d}}^{-1} & -\boldsymbol{\Phi}_{\mathrm{uu|d}}^{-1}\boldsymbol{\Phi}_{\mathrm{ud}}\boldsymbol{\Phi}_{\mathrm{dd}}^{-1} \\ * & * \end{bmatrix} ; \tag{B.48}$$

with $\boldsymbol{\Phi}_{\mathrm{uu|d}} = \boldsymbol{\Phi}_{\mathrm{uu}} - \boldsymbol{\Phi}_{\mathrm{ud}}\boldsymbol{\Phi}_{\mathrm{dd}}^{-1}\boldsymbol{\Phi}_{\mathrm{du}}$ (the *Schur complement* of $\boldsymbol{\Phi}_{\mathrm{dd}}$ in $\boldsymbol{\Phi}_{\bar{a}\bar{a}}$). On the other hand, we can write

$$\begin{aligned} \boldsymbol{\Phi}_{\bar{a}\bar{a}}^{-1} &= \frac{1}{\sigma_a^2}\boldsymbol{Z}^{-\mathsf{H}}\boldsymbol{Z}^{-1} = \frac{1}{\sigma_a^2}\boldsymbol{V}^{\mathsf{H}}\boldsymbol{V} \\ &= \frac{1}{\sigma_a^2}\begin{bmatrix} \boldsymbol{V}_{\mathrm{u}}^{\mathsf{H}}\boldsymbol{V}_{\mathrm{u}} & \boldsymbol{V}_{\mathrm{u}}^{\mathsf{H}}\boldsymbol{V}_{\mathrm{d}} \\ \boldsymbol{V}_{\mathrm{d}}^{\mathsf{H}}\boldsymbol{V}_{\mathrm{u}} & \boldsymbol{V}_{\mathrm{d}}^{\mathsf{H}}\boldsymbol{V}_{\mathrm{d}} \end{bmatrix} . \end{aligned} \tag{B.49}$$

A comparison of (B.48) and (B.49) reveals that

$$\boldsymbol{\Phi}_{\mathrm{uu|d}}^{-1} = \frac{1}{\sigma_a^2}\boldsymbol{V}_{\mathrm{u}}^{\mathsf{H}}\boldsymbol{V}_{\mathrm{u}} \tag{B.50}$$

$$-\boldsymbol{\Phi}_{\mathrm{uu|d}}^{-1}\boldsymbol{\Phi}_{\mathrm{ud}}\boldsymbol{\Phi}_{\mathrm{dd}}^{-1} = \frac{1}{\sigma_a^2}\boldsymbol{V}_{\mathrm{u}}^{\mathsf{H}}\boldsymbol{V}_{\mathrm{d}} \,. \tag{B.51}$$

Using these correspondences, the optimal linear estimator for $\bar{\boldsymbol{a}}_{\mathrm{u}}$ using $\bar{\boldsymbol{a}}_{\mathrm{d}}$ only (ignoring the receive vector $\boldsymbol{y}$) reads [105]

$$\begin{aligned} \boldsymbol{\mu}_{\mathrm{u|d}} &= \boldsymbol{\Phi}_{\mathrm{ud}}\boldsymbol{\Phi}_{\mathrm{dd}}^{-1}\bar{\boldsymbol{a}}_{\mathrm{d}} \\ &= -(\boldsymbol{V}_{\mathrm{u}}^{\mathsf{H}}\boldsymbol{V}_{\mathrm{u}})^{-1}(\boldsymbol{V}_{\mathrm{u}}^{\mathsf{H}}\boldsymbol{V}_{\mathrm{d}})^{-1}\,\bar{\boldsymbol{a}}_{\mathrm{d}} \,, \end{aligned} \tag{B.52}$$

and the covariance matrix of the error $\boldsymbol{e}_{\bar{a}_\mathrm{d}} = \boldsymbol{\mu}_{\mathrm{u|d}} - \bar{\boldsymbol{a}}_\mathrm{d}$ calculates to

$$\begin{aligned}\boldsymbol{\Phi}_{\mathrm{uu|d}} &= \boldsymbol{\Phi}_{\mathrm{uu}} - \boldsymbol{\Phi}_{\mathrm{ud}}\boldsymbol{\Phi}_{\mathrm{dd}}^{-1}\boldsymbol{\Phi}_{\mathrm{du}} \\ &= \sigma_a^2(\boldsymbol{V}_\mathrm{u}^\mathsf{H}\boldsymbol{V}_\mathrm{u})^{-1}\,. \end{aligned} \tag{B.53}$$

C) Now, the optimal linear MMSE estimator for $\bar{\boldsymbol{a}}_\mathrm{u}$ utilizing the knowledge from the receive vector $\boldsymbol{y}$ and the prediction calculated from $\bar{\boldsymbol{a}}_\mathrm{d}$ (these decisions are assumed to be perfectly known) can be given. For white noise ($\boldsymbol{\Phi}_{nn} = \sigma_n^2\boldsymbol{I}$, cf. (B.15); $\zeta = \sigma_n^2/\sigma_a^2$), it reads [105]

$$\begin{aligned}\tilde{\bar{\boldsymbol{a}}}_\mathrm{u} &= \left(\boldsymbol{W}_\mathrm{u}^\mathsf{H}\boldsymbol{\Phi}_{nn}^{-1}\boldsymbol{W}_\mathrm{u} + \boldsymbol{\Phi}_{\mathrm{uu|d}}^{-1}\right)^{-1}\boldsymbol{W}_\mathrm{u}^\mathsf{H}\boldsymbol{\Phi}_{nn}^{-1}\left(\tilde{\boldsymbol{y}} - \boldsymbol{W}_\mathrm{u}\boldsymbol{\mu}_{\mathrm{u|d}}\right) + \boldsymbol{\mu}_{\mathrm{u|d}} \\
&= \left(\boldsymbol{W}_\mathrm{u}^\mathsf{H}\boldsymbol{W}_\mathrm{u} + \zeta\boldsymbol{V}_\mathrm{u}^\mathsf{H}\boldsymbol{V}_\mathrm{u}\right)^{-1}\boldsymbol{W}_\mathrm{u}^\mathsf{H}\left(\boldsymbol{y} - \boldsymbol{W}_\mathrm{d}\bar{\boldsymbol{a}}_\mathrm{d} - \boldsymbol{W}_\mathrm{u}\boldsymbol{\mu}_{\mathrm{u|d}}\right) + \boldsymbol{\mu}_{\mathrm{u|d}} \\
&= \left(\boldsymbol{W}_\mathrm{u}^\mathsf{H}\boldsymbol{W}_\mathrm{u} + \zeta\boldsymbol{V}_\mathrm{u}^\mathsf{H}\boldsymbol{V}_\mathrm{u}\right)^{-1}\boldsymbol{W}_\mathrm{u}^\mathsf{H}\,\boldsymbol{y} \\
&\qquad - \left(\boldsymbol{W}_\mathrm{u}^\mathsf{H}\boldsymbol{W}_\mathrm{u} + \zeta\boldsymbol{V}_\mathrm{u}^\mathsf{H}\boldsymbol{V}_\mathrm{u}\right)^{-1}\boldsymbol{W}_\mathrm{u}^\mathsf{H}\boldsymbol{W}_\mathrm{d}\,\bar{\boldsymbol{a}}_\mathrm{d} \\
&\qquad - \left(\left(\boldsymbol{W}_\mathrm{u}^\mathsf{H}\boldsymbol{W}_\mathrm{u} + \zeta\boldsymbol{V}_\mathrm{u}^\mathsf{H}\boldsymbol{V}_\mathrm{u}\right)^{-1}\boldsymbol{W}_\mathrm{u}^\mathsf{H}\boldsymbol{W}_\mathrm{u} - \boldsymbol{I}\right)\boldsymbol{\mu}_{\mathrm{u|d}} \\
&= \left(\boldsymbol{W}_\mathrm{u}^\mathsf{H}\boldsymbol{W}_\mathrm{u} + \zeta\boldsymbol{V}_\mathrm{u}^\mathsf{H}\boldsymbol{V}_\mathrm{u}\right)^{-1}\boldsymbol{W}_\mathrm{u}^\mathsf{H}\,\boldsymbol{y} \\
&\qquad - \left(\boldsymbol{W}_\mathrm{u}^\mathsf{H}\boldsymbol{W}_\mathrm{u} + \zeta\boldsymbol{V}_\mathrm{u}^\mathsf{H}\boldsymbol{V}_\mathrm{u}\right)^{-1}\boldsymbol{W}_\mathrm{u}^\mathsf{H}\boldsymbol{W}_\mathrm{d}\,\bar{\boldsymbol{a}}_\mathrm{d} \\
&\qquad - \left(\boldsymbol{W}_\mathrm{u}^\mathsf{H}\boldsymbol{W}_\mathrm{u} + \zeta\boldsymbol{V}_\mathrm{u}^\mathsf{H}\boldsymbol{V}_\mathrm{u}\right)^{-1}\zeta\boldsymbol{V}_\mathrm{u}^\mathsf{H}\boldsymbol{V}_\mathrm{u}\,(\boldsymbol{V}_\mathrm{u}^\mathsf{H}\boldsymbol{V}_\mathrm{u})^{-1}(\boldsymbol{V}_\mathrm{u}^\mathsf{H}\boldsymbol{V}_\mathrm{d})^{-1}\,\bar{\boldsymbol{a}}_\mathrm{d} \\
&= \left(\boldsymbol{W}_\mathrm{u}^\mathsf{H}\boldsymbol{W}_\mathrm{u} + \zeta\boldsymbol{V}_\mathrm{u}^\mathsf{H}\boldsymbol{V}_\mathrm{u}\right)^{-1}\boldsymbol{W}_\mathrm{u}^\mathsf{H}\,\boldsymbol{y} \\
&\qquad - \left(\boldsymbol{W}_\mathrm{u}^\mathsf{H}\boldsymbol{W}_\mathrm{u} + \zeta\boldsymbol{V}_\mathrm{u}^\mathsf{H}\boldsymbol{V}_\mathrm{u}\right)^{-1}\left(\boldsymbol{W}_\mathrm{u}^\mathsf{H}\boldsymbol{W}_\mathrm{d} + \zeta\boldsymbol{V}_\mathrm{u}^\mathsf{H}\boldsymbol{V}_\mathrm{d}\right)\bar{\boldsymbol{a}}_\mathrm{d} \\
&= \underbrace{\left(\boldsymbol{\mathcal{W}}_\mathrm{u}^\mathsf{H}\boldsymbol{\mathcal{W}}_\mathrm{u}\right)^{-1}\boldsymbol{\mathcal{W}}_\mathrm{u}^\mathsf{H}}_{\boldsymbol{\mathcal{F}}_\mathrm{u}^{(l)}}\,\boldsymbol{y} - \underbrace{\left(\boldsymbol{\mathcal{W}}_\mathrm{u}^\mathsf{H}\boldsymbol{\mathcal{W}}_\mathrm{u}\right)^{-1}\boldsymbol{\mathcal{W}}_\mathrm{u}^\mathsf{H}\,\boldsymbol{\mathcal{W}}_\mathrm{d}}_{\boldsymbol{B}_\mathrm{u}^{(l)}}\,\bar{\boldsymbol{a}}_\mathrm{d}\,,\end{aligned} \tag{B.54}$$

and the correlation matrix of the estimation error $\tilde{\boldsymbol{n}} \overset{\mathrm{def}}{=} \check{\boldsymbol{a}}_\mathrm{u}^{(K)} - \bar{\boldsymbol{a}}_\mathrm{u}$, is given by [105]

$$\begin{aligned}\boldsymbol{\Phi}_{ee} &= \left(\boldsymbol{W}_\mathrm{u}^\mathsf{H}\boldsymbol{\Phi}_{nn}^{-1}\boldsymbol{W}_\mathrm{u} + \boldsymbol{\Phi}_{\mathrm{uu|d}}^{-1}\right)^{-1} \\ &= \sigma_n^2\left(\boldsymbol{W}_\mathrm{u}^\mathsf{H}\boldsymbol{W}_\mathrm{u} + \zeta\boldsymbol{V}_\mathrm{u}^\mathsf{H}\boldsymbol{V}_\mathrm{u}\right)^{-1} \\ &= \sigma_n^2\left(\boldsymbol{\mathcal{W}}_\mathrm{u}^\mathsf{H}\boldsymbol{\mathcal{W}}_\mathrm{u}\right)^{-1}\,. \end{aligned} \tag{B.55}$$

From these results, we see the following important fact: having already fixed the integer matrix $\boldsymbol{Z}$ (and hence the parts $\boldsymbol{V}_{\mathrm{u}}$ and $\boldsymbol{V}_{\mathrm{d}}$), the optimal receive matrix is given by $\boldsymbol{\mathcal{F}}_{\mathrm{u}}^{(l)} = \boldsymbol{\mathcal{W}}_{\mathrm{u}}^{+}$, i.e., the pseudoinverse of the left part of the reduced augmented channel matrix. Since this matrix contains $\boldsymbol{V}_{\mathrm{u}}$ as lower part, the correlations are taken correctly into account. Moreover, the prediction from the already detected/decoded linear combinations is subsumed into the feedback matrix $\boldsymbol{B}_{\mathrm{u}}^{(l)} = \boldsymbol{\mathcal{W}}_{\mathrm{u}}^{+}\boldsymbol{\mathcal{W}}_{\mathrm{d}}$. Hence, in summary, using augmented matrices where the lower part reflects the correlations of the symbols, the MMSE estimator and the correlation matrix of the estimation error are simply given by the respective (pseudo)inverse (cf. also [40]).

However, up to now we have assumed a given integer matrix $\boldsymbol{Z}$ which also determines $\boldsymbol{V}_{\mathrm{u}}$ and $\boldsymbol{V}_{\mathrm{d}}$. For best performance, and since in the current iteration step l we are only interested in a single linear combination, the l present combinations can further be combined by integer scaling factors. Defining $\boldsymbol{z}_{\mathrm{u},l} = [z_1, \ldots, z_l]^{\mathsf{T}}$, the estimate is calculated from (B.54) as

$$
\begin{aligned}
\tilde{\bar{a}}_l &= \boldsymbol{z}_{\mathrm{u},l}^{\mathsf{H}} \tilde{\bar{\boldsymbol{a}}}_{\mathrm{u}} \\
&= \boldsymbol{z}_{\mathrm{u},l}^{\mathsf{H}} \boldsymbol{\mathcal{W}}_{\mathrm{u}}^{+}\, \boldsymbol{\mathcal{y}} - \boldsymbol{z}_{\mathrm{u},l}^{\mathsf{H}} \boldsymbol{\mathcal{W}}_{\mathrm{u}}^{+} \boldsymbol{\mathcal{W}}_{\mathrm{d}}\, \bar{\boldsymbol{a}}_{\mathrm{d}}\,,
\end{aligned}
\tag{B.56}
$$

and the estimation variance amounts to

$$
\begin{aligned}
\sigma_e^2 &= \sigma_n^2\, \boldsymbol{z}_{\mathrm{u},l}^{\mathsf{H}} \left(\boldsymbol{\mathcal{W}}_{\mathrm{u}}^{\mathsf{H}} \boldsymbol{\mathcal{W}}_{\mathrm{u}}\right)^{-1} \boldsymbol{z}_{\mathrm{u},l} \\
&= \sigma_n^2\, ||(\boldsymbol{\mathcal{W}}_{\mathrm{u}}^{+})^{\mathsf{H}} \boldsymbol{z}_{\mathrm{u},l}||^2\,.
\end{aligned}
\tag{B.57}
$$

Thus, the optimal next integer vector—which is of dimension l and an increment to the already present integer combinations—is given by a *shortest vector problem* in the lattice spanned by $(\boldsymbol{\mathcal{W}}_{\mathrm{u}}^{+})^{\mathsf{H}}$ (the dual lattice to that spanned by $\boldsymbol{\mathcal{W}}_{\mathrm{u}}$). The matrix $\boldsymbol{Z}$ has to be updated adequately (details are given below). The l^{th} row of the feedforward matrix $\boldsymbol{\mathcal{F}}$ and the feedback matrix $\boldsymbol{B}$ are given by

$$
\boldsymbol{z}_{\mathrm{u},l}^{\mathsf{H}} \boldsymbol{\mathcal{W}}_{\mathrm{u}}^{+}\,, \qquad [\underbrace{0, \ldots, 0}_{l-1 \text{ zeros}}, 1, \boldsymbol{z}_{\mathrm{u},l}^{\mathsf{H}} \boldsymbol{\mathcal{W}}_{\mathrm{u}}^{+} \boldsymbol{\mathcal{W}}_{\mathrm{d}}]\,,
\tag{B.58}
$$

respectively.

Due to the specific calculation of $\boldsymbol{\mathcal{F}}_{\mathrm{u}}^{(l)}$ we have

$$
\boldsymbol{\mathcal{F}}_{\mathrm{u}} \boldsymbol{\mathcal{W}}^{(l)} = (\boldsymbol{\mathcal{W}}_{\mathrm{u}})^{+} [\boldsymbol{\mathcal{W}}_{\mathrm{u}}\ \boldsymbol{\mathcal{W}}_{\mathrm{d}}]
$$

$$= [\boldsymbol{I} \quad \boldsymbol{X}] \tag{B.59}$$

where $\boldsymbol{X}$ still has to be specified. Moreover, since equalization is done only w.r.t. the not yet detected linear combinations

$$\boldsymbol{\mathcal{F}}_{\mathrm{d}}^{(l)} \boldsymbol{\mathcal{W}}^{(l)} = [\boldsymbol{0} \;\; \boldsymbol{R}_{\mathrm{d}}] \,, \tag{B.60}$$

where $\boldsymbol{R}_{\mathrm{d}}$ is an upper triangular matrix with unit main diagonal. Hence, taking (B.45) into account, in total

$$\begin{bmatrix} \boldsymbol{\mathcal{F}}_{\mathrm{u}} \\ \boldsymbol{\mathcal{F}}_{\mathrm{d}} \end{bmatrix} \boldsymbol{\mathcal{H}} (\boldsymbol{Z}^{(l)})^{-1} = \begin{bmatrix} \boldsymbol{I} & \boldsymbol{X} \\ \boldsymbol{0} & \boldsymbol{R}_{\mathrm{d}} \end{bmatrix} . \tag{B.61}$$

According to (B.6), the rows of $\boldsymbol{\mathcal{F}}_{\mathrm{d}}^{(l)}$ are orthogonal to that of $\boldsymbol{\mathcal{F}}_{\mathrm{u}}^{(l)}$. In the final step, we arrive at

$$\boldsymbol{\mathcal{F}} \boldsymbol{\mathcal{H}} \boldsymbol{Z}^{-1} = \boldsymbol{R} \,, \tag{B.62}$$

where $\boldsymbol{\mathcal{F}}$ has orthogonal rows and $\boldsymbol{R}$ is an upper triangular matrix. Thus, over the iterations, the procedure induces a QR decomposition of the channel matrix multiplied by the inverse of the integer matrix.

B.3.2 Dual-Lattice Approach

Similar to the V-BLAST algorithm, the above procedure results in the optimal (w.r.t. worst-link performance [117]) integer matrix and corresponding feedforward and feedback matrices. However, it requires a large effort as repeatedly pseudoinverses have to be calculated. As above, a dual-lattice approach is very well suited to overcome this problem.

In the dual-lattice approach, the Hermitian of the pseudoinverse of the augmented channel matrix is calculated

$$(\boldsymbol{\mathcal{H}}^{+})^{\mathsf{H}} = ((\boldsymbol{\mathcal{H}}^{\mathsf{H}} \boldsymbol{\mathcal{H}})^{-1} \boldsymbol{\mathcal{H}}^{\mathsf{H}})^{\mathsf{H}} = \boldsymbol{\mathcal{H}} (\boldsymbol{\mathcal{H}}^{\mathsf{H}} \boldsymbol{\mathcal{H}})^{-1} \tag{B.63}$$

and a generalized version of the Gram–Schmidt procedure (cf. [38]) is carried out leading to

$$(\boldsymbol{\mathcal{H}}^{+})^{\mathsf{H}} \boldsymbol{Z}^{\mathsf{H}} = \boldsymbol{\mathcal{Q}} \boldsymbol{L} \,, \tag{B.64}$$

where $\boldsymbol{\mathcal{Q}}$ has orthogonal columns, $\boldsymbol{L}$ is *lower* triangular with unit main-diagonal, and $\boldsymbol{Z}$ is an integer matrix with $\boldsymbol{Z}^{\mathsf{H}} = [\boldsymbol{z}_1, \ldots, \boldsymbol{z}_K]$. We now show by mathematical induction that these matrices are related to that of the above direct procedure as $\boldsymbol{\mathcal{Q}}^{\mathsf{H}} = \boldsymbol{\mathcal{F}}$ and $\boldsymbol{L}^{-\mathsf{H}} = \boldsymbol{R}$ and that the same integer matrix $\boldsymbol{Z}$ is obtained.

Base Case

For $l = K$, the initialization is given by

$$\boldsymbol{\mathcal{Q}}^{(K)} = (\boldsymbol{\mathcal{H}}^{+})^{\mathsf{H}}, \qquad \boldsymbol{Z}^{(K)} = \boldsymbol{I}, \qquad \boldsymbol{L}^{(K)} = \boldsymbol{I}, \tag{B.65}$$

and we search for an integer vector $\boldsymbol{z}_K$, such that $\boldsymbol{\mathcal{Q}}^{(K)}\boldsymbol{z}_K$ has the *smallest* norm. This (squared) norm is given by

$$||\boldsymbol{\mathcal{Q}}^{(K)}\boldsymbol{z}_K||^2 = \boldsymbol{z}_K^{\mathsf{H}}\boldsymbol{\mathcal{H}}^{+}(\boldsymbol{\mathcal{H}}^{+})^{\mathsf{H}}\boldsymbol{z}_K, \tag{B.66}$$

which is the same criterion as in (B.43). Hence the same integer vector as in the direct approach is found—which is the shortest vector in the lattice spanned by $(\boldsymbol{\mathcal{H}}^{+})^{\mathsf{H}}$, which is the dual lattice to that spanned by $\boldsymbol{\mathcal{H}}$ (cf. Sec. A.1), hence the denomination *"dual-lattice approach"*.

The integer vector $\boldsymbol{z}_K^{\mathsf{H}}$ is recorded as the last column of $\boldsymbol{Z}^{\mathsf{H}}$ and the last column of $\boldsymbol{\mathcal{Q}}$ is updated to $(\boldsymbol{\mathcal{H}}^{+})^{\mathsf{H}}\boldsymbol{z}_K$. Both columns are never changed during the following process. As will be explained below, the other columns of $\boldsymbol{Z}^{\mathsf{H}}$ and $\boldsymbol{\mathcal{Q}}$ might also have to be updated at this point. Finally, a Gram–Schmidt orthogonalization of the last column of $\boldsymbol{\mathcal{Q}}$ against the others is performed. Thereby, the last row of $\boldsymbol{L}$ is generated.

Induction Step

In iteration l, since GSO is performed, we have

$$\begin{aligned}(\boldsymbol{\mathcal{H}}^{+})^{\mathsf{H}}(\boldsymbol{Z}^{\mathsf{H}})^{(l)} &= \boldsymbol{\mathcal{Q}}^{(l)}\boldsymbol{L}^{(l)} \\ &= [\boldsymbol{\mathcal{Q}}_{\mathrm{u}}\ \boldsymbol{\mathcal{Q}}_{\mathrm{d}}]\begin{bmatrix}\boldsymbol{I} & \boldsymbol{0} \\ \boldsymbol{X} & \boldsymbol{L}_{\mathrm{d}}\end{bmatrix}\end{aligned} \tag{B.67}$$

where the columns of $\boldsymbol{\mathcal{Q}}_{\mathrm{d}}$ are orthogonal to each other and to that of $\boldsymbol{\mathcal{Q}}_{\mathrm{u}}$, $\boldsymbol{L}_{\mathrm{d}}$ is lower triangular with unit main diagonal, and $\boldsymbol{X}$ needs not to be specified.

Assume (induction) that $\boldsymbol{\mathcal{F}}_{\mathrm{d}} = (\boldsymbol{\mathcal{Q}}_{\mathrm{d}})^{\mathsf{H}}$ and the Hermitian of the integer matrix, $\boldsymbol{Z}^{\mathsf{H}}$, are the same in both approaches. Then, the reduced augmented channel matrix $\boldsymbol{\mathcal{W}}^{(l)} = \boldsymbol{\mathcal{H}}(\boldsymbol{Z}^{(l)})^{-1} = [\boldsymbol{\mathcal{W}}_\mathrm{u}\ \boldsymbol{\mathcal{W}}_\mathrm{d}]$ is the same as in the direct approach. Moreover, since in the direct approach the next estimation matrix is $\boldsymbol{\mathcal{F}}_\mathrm{u} = \boldsymbol{\mathcal{W}}_\mathrm{u}^+$ and, as shown in Sec. B.1, a Gram–Schmidt orthogonalization on $\boldsymbol{\mathcal{Q}}$ results in $\boldsymbol{\mathcal{Q}}_\mathrm{u} = (\boldsymbol{\mathcal{W}}_\mathrm{u}^+)^\mathsf{H}$, we conclude that $\boldsymbol{\mathcal{F}}_\mathrm{u} = \boldsymbol{\mathcal{Q}}_\mathrm{u}^\mathsf{H}$.

In classical DFE the column with the smallest norm in $\boldsymbol{\mathcal{Q}}_\mathrm{u}$ is selected at this step. In contrast, in LRA DFE, the next best integer linear combination of the rows of $\boldsymbol{\mathcal{Q}}_\mathrm{u}$ is determined. This is identical to searching for the shortest vector in the lattice spanned by this matrix, i.e.,

$$\boldsymbol{z}_\mathrm{s} = \underset{\boldsymbol{z}_{\mathrm{u},l} \in \mathbb{G}^l}{\operatorname{argmin}} \, ||\boldsymbol{\mathcal{Q}}_\mathrm{u} \boldsymbol{z}_{\mathrm{u},l}||^2 \,, \tag{B.68}$$

which is the same problem as (B.57) and hence the same integer vector $\boldsymbol{z}_{\mathrm{u},l} = [z_1, \ldots, z_l]^\mathsf{T}$ will be found.

Consequently, due to induction, both approaches lead to the same integer matrix $\boldsymbol{Z}$ and feedforward matrix $\boldsymbol{\mathcal{F}} = \boldsymbol{\mathcal{Q}}^\mathsf{H}$, respectively, and also to the same feedback matrix $\boldsymbol{B} = \boldsymbol{L}^{-\mathsf{H}}$, which can be seen when solving (B.67) for $\boldsymbol{L}^{-\mathsf{H}}$

$$\begin{aligned} \boldsymbol{L}^{-\mathsf{H}} &\overset{(\mathrm{B.67})}{=} \left(\boldsymbol{\mathcal{Q}}^+ (\boldsymbol{\mathcal{H}}^+)^\mathsf{H} \boldsymbol{Z}^\mathsf{H}\right)^{-\mathsf{H}} \\ &= \left(\boldsymbol{\mathcal{H}}^+ (\boldsymbol{\mathcal{Q}}^+)^\mathsf{H}\right)^+ \boldsymbol{Z}^{-1} \\ &= \boldsymbol{\mathcal{Q}}^\mathsf{H} \boldsymbol{\mathcal{H}} \boldsymbol{Z}^{-1} \\ &\overset{(\mathrm{B.62})}{=} \boldsymbol{B} \,. \end{aligned} \tag{B.69}$$

Finally, we have to discuss how $\boldsymbol{Z}$ and $\boldsymbol{\mathcal{Q}}$ are updated in iteration l. The main aim is to place $\boldsymbol{q}_\mathrm{s} \overset{\mathrm{def}}{=} \boldsymbol{\mathcal{Q}}_\mathrm{u} \boldsymbol{z}_\mathrm{s}$ as l^th column in $\boldsymbol{\mathcal{Q}}$. In order that (B.67) is still satisfied, $\boldsymbol{Z}^\mathsf{H}$ has to be changed, too, and $\boldsymbol{z}_{\mathrm{u},l}$ cannot be placed directly in the integer matrix. Instead, the update can be written as[5]

$$(\boldsymbol{\mathcal{H}}^+)^\mathsf{H} \underbrace{(\boldsymbol{Z}^\mathsf{H})^{(l)} \boldsymbol{U}^{(l)}}_{(\boldsymbol{Z}^\mathsf{H})^{(l-1)}} = \underbrace{\boldsymbol{\mathcal{Q}}^{(l)} \boldsymbol{U}^{(l)}}_{\boldsymbol{\mathcal{Q}}^{(l-1)}} \underbrace{(\boldsymbol{U}^{(l)})^{-1} \boldsymbol{L}^{(l)} \boldsymbol{U}^{(l)}}_{\boldsymbol{L}^{(l-1)}} \,, \tag{B.70}$$

[5]Since the left multiplication with $(\boldsymbol{U}^{(l)})^{-1}$ acts only on the upper l rows of $\boldsymbol{L}$ which, however, have not been calculated yet, the right multiplication with $\boldsymbol{U}^{(l)}$ is sufficient for the update of $\boldsymbol{L}$, cf. also [38].

where
$$\boldsymbol{U}^{(l)} = \begin{bmatrix} \boldsymbol{U}_{\mathrm{u}}^{(l)} & \boldsymbol{0} \\ \boldsymbol{0} & \boldsymbol{I} \end{bmatrix} , \tag{B.71}$$

with $l \times l$ part $\boldsymbol{U}_{\mathrm{u}}^{(l)}$, acts on the left l columns.

In order that $\boldsymbol{Z}^{\mathsf{H}}$ remains integer, $\boldsymbol{U}^{(l)}$ and thus $\boldsymbol{U}_{\mathrm{u}}^{(l)}$ have to be integer as well. Moreover, $\boldsymbol{U}^{(l)}$ and thus $\boldsymbol{U}_{\mathrm{u}}^{(l)}$ have to be *unimodular*, i.e., $|\det(\boldsymbol{U}_{\mathrm{u}}^{(l)})| = 1$. This can be seen from the following fact: In the next iteration (number $l-1$) the shortest vector in the lattice spanned by the left $l-l$ columns of $\boldsymbol{\mathcal{Q}}^{(l-1)} = \boldsymbol{\mathcal{Q}}^{(l)}\boldsymbol{U}^{(l)}$ has to be determined. If the update is not unimodular, a sublattice of $\boldsymbol{\mathcal{Q}}^{(l)}$ would be present. This, however, poses restrictions for the further steps as a shortest vector in a thinned lattice is searched which may result in a longer vector and thus poorer performance. Hence, in LRA DFE unimodular updates should be performed, finally leading in an optimal way to a unimodular integer matrix. This fact that in LRA DFE we can restrict ourselves to unimodular matrices and hence solving a lattice reduction problem has already been observed in [94], cf. also [117].

Still the update matrix $\boldsymbol{U}^{(l)}$ has to be determined. In [155] a very efficient strategy for the update (implicitly obtaining $\boldsymbol{U}^{(l)}$) has been proposed. The idea is to successively modify adjacent columns such that after $l-1$ steps column l of $\boldsymbol{\mathcal{Q}}^{(l)}$ contains the shortest vector $\boldsymbol{q}_{\mathrm{s}} = \boldsymbol{\mathcal{Q}}_{\mathrm{u}}\boldsymbol{z}_{\mathrm{s}}$. In [155] this has been only shown over the integers $\mathbb{Z}$, but the strategy also applies to the Gaussian integers $\mathbb{G}$ and the Eisenstein integers $\mathbb{E}$ since they constitute Euclidean rings [117].

We start[6] at $u = 1$ and successively calculate integers c_1 and c_2 via the *extended Euclidean algorithm* [49] such that for the coordinates $\boldsymbol{z}_{\mathrm{s}} = [z_1, \ldots, z_l]^{\mathsf{T}}$ of the shortest vector the equation

$$c_1\, z_u + c_2\, z_{u+1} = g \overset{\text{def}}{=} \gcd(z_u, z_{u+1}) , \tag{B.72}$$

holds, where $\gcd(\cdot,\cdot)$ denotes the greatest common divisor. It is easy to see that the $l \times l$ matrix

$$\boldsymbol{U}_{2,u} = \begin{bmatrix} \boldsymbol{I}_{u-1} & & \boldsymbol{0} \\ & \boldsymbol{U}_{\mathrm{u},2,u} & \\ \boldsymbol{0} & & \boldsymbol{I}_{l-u-1} \end{bmatrix} , \quad \text{with} \quad \boldsymbol{U}_{\mathrm{u},2,u} = \begin{bmatrix} c_2 & z_u/g \\ -c_1 & z_{u+1}/g \end{bmatrix} \tag{B.73}$$

[6] Since we proceed from $l = K$ to $l = 1$, the update has to be done from $u = 1$ to $u = l - 1$. This is the reverse order as given in [155].

is unimodular integer and its inverse has the same structure but with $\boldsymbol{U}_{\mathrm{u},2,u}$ replaced by the inverse $\boldsymbol{U}_{\mathrm{u},2,u}^{-1} = \left[\begin{smallmatrix} z_{u+1}/g & -z_u/g \\ c_1 & c_2 \end{smallmatrix}\right]$. Since

$$\boldsymbol{\mathcal{Q}}_{\mathrm{u}} \boldsymbol{z}_{\mathrm{s}} = \boldsymbol{\mathcal{Q}}_{\mathrm{u}} \boldsymbol{U}_{2,u} \boldsymbol{U}_{2,u}^{-1} \boldsymbol{z}_{\mathrm{s}} \tag{B.74}$$

and

$$\boldsymbol{U}_{\mathrm{u},2,u}^{-1} \begin{bmatrix} z_u \\ z_{u-1} \end{bmatrix} = \begin{bmatrix} z_{u+1}/g & -z_u/g \\ c_1 & c_2 \end{bmatrix} \begin{bmatrix} z_u \\ z_{u+1} \end{bmatrix} = \begin{bmatrix} 0 \\ g \end{bmatrix} \tag{B.75}$$

each application of $\boldsymbol{U}_{2,u}$ forces the next top entry to zero. For the next iteration z_{u+1} is set to g (cf. (B.72)). At step $u = l-1$ the final right-hand-side vector is the l^{th} unit vector, hence, column l in $\boldsymbol{\mathcal{Q}}_{\mathrm{u}}$ equals the shortest vector. The update matrix in (B.70) then equals $\boldsymbol{U}_{\mathrm{u}}^{(l)} = \boldsymbol{U}_{2,1} \cdot \boldsymbol{U}_{2,2} \cdots \boldsymbol{U}_{2,l-1}$.

In summary, the optimal equalization matrices for LRA DFE can be calculated by a Gram-Schmidt orthogonalization procedure and a search for the shortest vector in lattices of successively decreasing dimension. Thereby, the complexity is dominated by the shortest vector algorithm. A more efficient realization can be obtained if (suboptimal, low-complexity) lattice reduction (e.g., via the LLL algorithm) is applied as preprocessing.

Noteworthy, the presented dual-lattice approach is equal to the Hermite–Korkine–Zolotareff (HKZ) reduction algorithm, except that the size reduction step is not applied [94, 116]. Size reduction operates on the integer matrix $\boldsymbol{Z}$ and the lower triangular matrix $\boldsymbol{L}$ only. As for noise enhancement only the column norms of $\boldsymbol{\mathcal{Q}}$ are relevant and this matrix is not touched by size reduction, (almost) no change in performance[7] is caused.

[7] As size reduction lowers the magnitudes of the entries of $\boldsymbol{L}$, the magnitudes of the entries of $\boldsymbol{Z}$ may be increased. This, however, might lead to a somewhat larger error multiplication in the recovery of the data streams via $\boldsymbol{Z}^{-1}$.

C

Implementation Issues

In this appendix, some practical issues when implementing LRA/IF equalization schemes are collected. This includes the handling of offsets usually present in signal constellations and effects due to individual decoding and signal recovery via the inverse of the integer matrix.

C.1 Signal Constellations

In Chapter 2, the constituent signal constellation $\mathcal{A}$ is defined in two different ways, which both have their theoretical and practical relevance. In (2.1) the constellation is given starting from the underlying signal-point lattice $\mathbf{\Lambda}_{\mathrm{a}}$; from it the constellation is carved out via the intersection with the Voronoi region of the boundary lattice. This definition focuses on the lattice structure of the constellation but ignores practical aspects. For example, conventional QAM/ASK constellations usually do not include the origin as signal point, hence a translate of a lattice is used as signal-point lattice. In addition, no labeling of signal points is associated with this definition.

This shortcoming is resolved with the second definition by specifying a particular mapping (2.7); the constellation is then obtained as

$$\mathcal{A} = \left\{ \mathcal{M}(\mathfrak{b}_{m-1} \dots \mathfrak{b}_1 \mathfrak{b}_0) \mid \mathfrak{b}_l \in \mathbb{F}_2, l = 0, \dots, m-1 \right\} . \qquad \text{(C.1)}$$

In this definition the offset O to obtain zero-mean constellations is explicitly given. In Fig. C.1 the generation of a 16QAM constellation using the mapping (2.7) ($M = 16$, $B = (-1+\mathrm{j})^4 = -4$, $O = (1+\mathrm{j})/2$) and in Fig. C.2 the generation of a 32QAM constellation $M = 32$, $B = (-1+\mathrm{j})^5 = 4-4\mathrm{j}$, $O = -1/2$) are exemplarily depicted.[1]

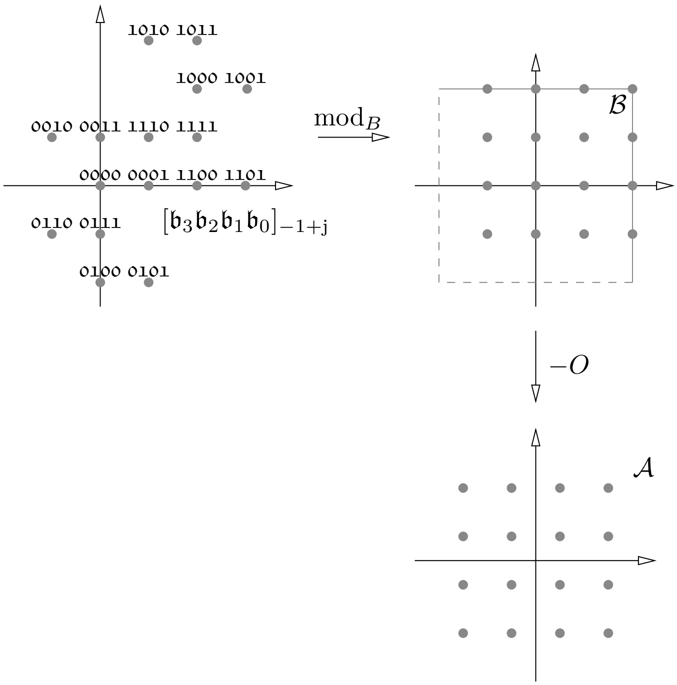

Figure C.1: Generation of a 16QAM constellation using the mapping (2.7).

In practical systems, especially when dealing with integer linear combinations, this offset and the actual boundary of the constellation have to be handled suitably.

[1]Thereby ties in the rounding to the nearest integer in the definition of mod_B are resolved towards $-\infty$ in real and imaginary part. Hence in $\mathrm{mod}_{-4}(x) = x - (-4)\lfloor x\,(-4)/(|-4|^2)\rceil = x + 4\lfloor -x\,/4\rceil$ ties are resolved towards $+\infty$.

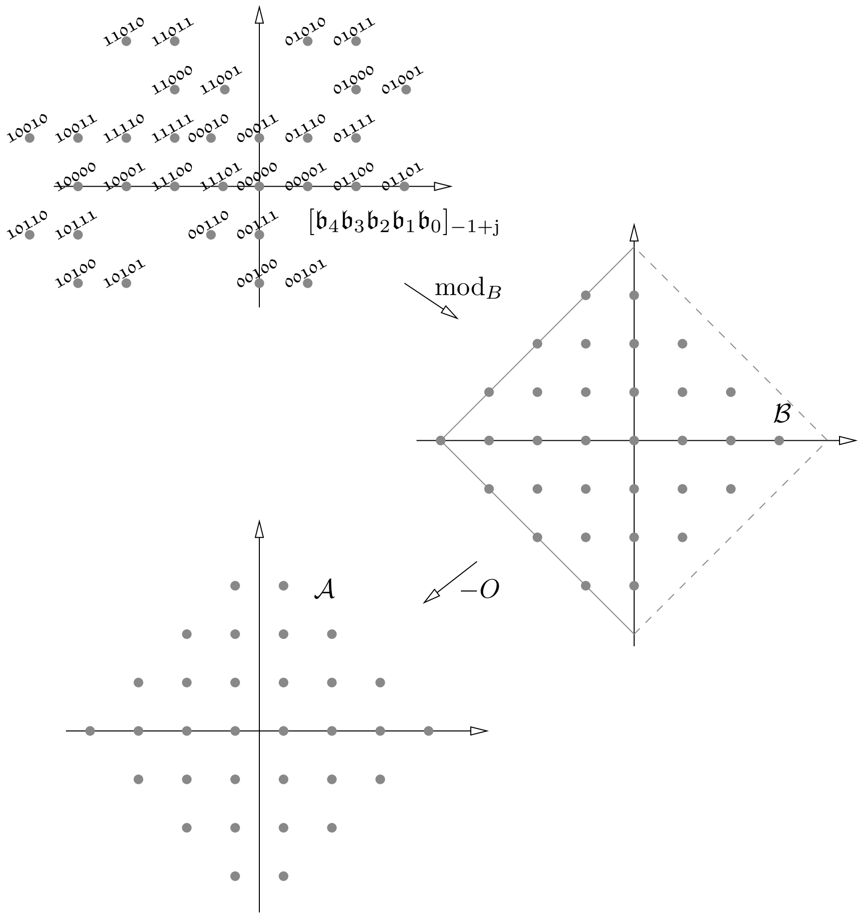

Figure C.2: Generation of a 32QAM constellation using the mapping (2.7).

Defining the region (gray bordered in Fig. C.1) induced by the remainder operation (cf. Appendix D) by

$$\mathcal{B} \stackrel{\text{def}}{=} \left\{ \text{mod}_B(x) \mid x \in \begin{cases} \mathbb{R}, & \text{ASK} \\ \mathbb{C}, & \text{QAM} \end{cases} \right\} \tag{C.2}$$

the elements of $\mathcal{A}$ in (C.1), hence the transmit symbols, are drawn from $\left(\boldsymbol{\Lambda}_{\rm a} = \begin{cases} \mathbb{Z}, & \text{ASK} \\ \mathbb{G}, & \text{QAM} \end{cases}\right)$

$$a \in (\boldsymbol{\Lambda}_{\rm a} \cap \mathcal{B}) - O \;\subset\; \boldsymbol{\Lambda}_{\rm a} - O\,. \tag{C.3}$$

The receive vector is given as (cf. (2.12) and (3.1))

$$\begin{aligned} \boldsymbol{y} &= \boldsymbol{H}\boldsymbol{a} + \boldsymbol{n} \\ & \boldsymbol{W}\boldsymbol{Z}\boldsymbol{a} + \boldsymbol{n} \,, \end{aligned} \tag{C.4}$$

where $\boldsymbol{Z} = [\, z_{l,k} \,] \in \begin{cases} \mathbb{Z}^{K \times K}, & \text{ASK} \\ \mathbb{G}^{K \times K}, & \text{QAM} \end{cases}$. Since $\boldsymbol{Z}\boldsymbol{\Lambda}_{\mathrm{a}}^{K} = \boldsymbol{\Lambda}_{\mathrm{a}}^{K}$, the vector $\bar{\boldsymbol{a}} = \boldsymbol{Z}\boldsymbol{a}$ of integer linear combinations of the data symbols is drawn from

$$\bar{\boldsymbol{a}} \;=\; \boldsymbol{Z}\boldsymbol{a} \in \boldsymbol{Z}(\boldsymbol{\Lambda}_{\mathrm{a}} - O)^{K} \;=\; \boldsymbol{\Lambda}_{\mathrm{a}}^{K} - O\boldsymbol{Z}\boldsymbol{1} \,, \tag{C.5}$$

where $\boldsymbol{1}$ is the all-ones vector of dimension K. The elements of $\bar{\boldsymbol{a}}$ are thus drawn from the signal-point lattice with an offset determined by the row sum over the integer matrix $\boldsymbol{Z}$, i.e.,

$$\text{with} \qquad \begin{aligned} \bar{a}_l &\in \boldsymbol{\Lambda}_{\mathrm{a}}^{K} - O_l \\ O_l &\stackrel{\text{def}}{=} O \sum_{k=1}^{K} z_{l,k} \,. \end{aligned} \qquad l = 1, \ldots, K \tag{C.6}$$

When employing LRA/IF linear equalization, the decoders see the signal

$$\boldsymbol{r} \;=\; \boldsymbol{Z}\boldsymbol{a} + \tilde{\boldsymbol{n}} \;=\; \bar{\boldsymbol{a}} + \tilde{\boldsymbol{n}} \,. \tag{C.7}$$

Hence, when the decoders work on the (non-shifted) lattice $\boldsymbol{\Lambda}_{\mathrm{a}}$ (more precisely, the coding lattice $\boldsymbol{\Lambda}_{\mathrm{c}}$ based thereon) the offset O_l has to be eliminated (by adding O_l) prior to the decoders. The individual offsets O_l have to be subtracted again at the decoder outputs (the decoders deliver the codewords in signal space), prior to resolving the integer interference (cf. Fig. 3.1). This ensures that the inverse mapping sees the usual zero-mean constellation. Alternatively, since $\boldsymbol{Z}^{-1} O\boldsymbol{Z}\boldsymbol{1} = O\boldsymbol{1}$, the common offset O has to be subtracted from all symbol estimates after applying the inverse integer matrix.

Using LRA decision-feedback equalization (cf. Chapter 5), the receive vector after the feedforward matrix (cf. Fig. 5.1) is given by

$$\boldsymbol{r} \;=\; \boldsymbol{B}\boldsymbol{Z}\boldsymbol{a} + \tilde{\boldsymbol{n}} \;=\; \boldsymbol{B}\bar{\boldsymbol{a}} + \tilde{\boldsymbol{n}} \,, \tag{C.8}$$

where the feedback matrix $\boldsymbol{B}$ is upper triangular with unit main diagonal. Decisions are taken successively in sequence $l = K, \ldots, 1$. When correct decoding results $\bar{a}_\ell$, $\ell = l+1,\ldots,K$, are fed back and subtracted from $\boldsymbol{r}$ (via $\boldsymbol{B} - \boldsymbol{I}$), in step l the signal $\bar{a}_l + \tilde{n}_l$ is the input to the decoder; hence the same offset O_l as in case of the linear equalization is present. In summary, as above, the offsets O_l have to be added at the input of the decoders and subtracted from the decoding results.

The same considerations are also valid for Eisenstein constellations generated using the mapping function (2.10). An example for a 27-ary constellation ($M = 27$, $m = 3$, $\phi = -1+\omega$, $B = \phi^3 = 3\sqrt{3}\mathrm{j}$) is depicted in Fig. C.3.

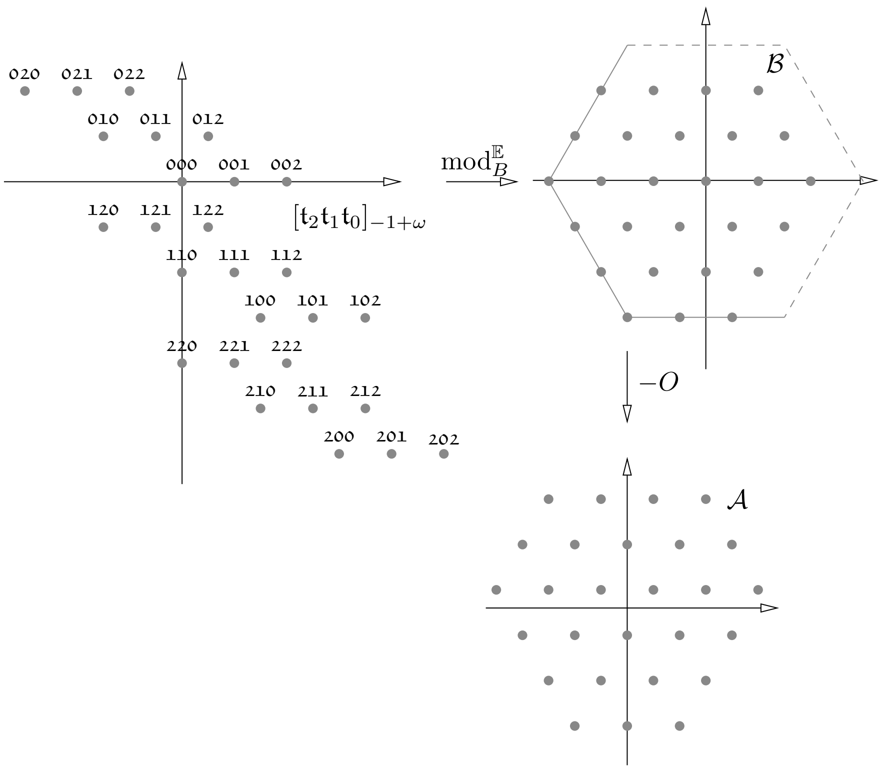

Figure C.3: Generation of a 27-ary Eisenstein constellation using the mapping (2.10).

C.2 Decoding

One of the main features in LRA/IF equalization is that joint equalization is only performed for the non-integer part $\boldsymbol{W}$ of the channel, cf. Sec. 3.1. Then, individual, parallel decoding of the K integer linear combinations takes place, cf. Fig. 3.1. This approach leads to low-complexity high-performing schemes but also some issues which have to be kept in mind in practical implementations.

For illustration purpose let us assume real-valued signaling employing 4ASK per component (user). We expect the offsets of the constellations to be already eliminated, hence the signal points a_k are drawn from the set $\mathbb{Z}_4 \overset{\text{def}}{=} \{0, 1, 2, 3\}$. Moreover, let $K = 2$. When plotting the first component, a_1, on the horizontal axis and the second component, a_2, on the vertical axis, the transmit constellation, all vectors $\boldsymbol{a} = \begin{bmatrix} a_1 \\ a_2 \end{bmatrix} \in \mathbb{Z}_4^2$, is then given by the 4 by 4 arrangement (resembling 16QAM) depicted on the left-hand side of Fig. C.4.

Let the integer matrix be $\boldsymbol{Z} = \begin{bmatrix} 1 & 1 \\ 0 & 1 \end{bmatrix}$. Then the vectors of integer linear combinations, on which decoding is based, $\bar{\boldsymbol{a}} = \boldsymbol{Z}\boldsymbol{a} \in \boldsymbol{Z}\mathbb{Z}_4^2$, form the arrangement shown on the left-hand side of Fig. C.4.

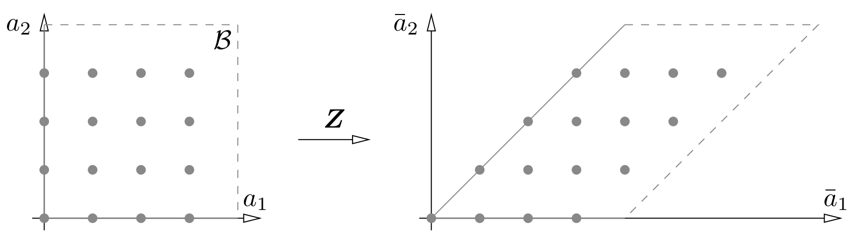

Figure C.4: Action of the integer matrix $\boldsymbol{Z} = \begin{bmatrix} 1 & 1 \\ 0 & 1 \end{bmatrix}$ on the data vectors $\boldsymbol{a} \in \mathbb{Z}_4^2$.

Since individual decoding/detection of these linear combinations is performed, the actual boundary region of the set of $\bar{\boldsymbol{a}}$ is not taken into account [142]. Consequently, non-valid vectors $\hat{\bar{\boldsymbol{a}}}$ outside the boundary can be delivered. After application of the inverse integer matrix, here $\boldsymbol{Z}^{-1} = \begin{bmatrix} 1 & -1 \\ 0 & 1 \end{bmatrix}$, these points $\hat{\boldsymbol{a}}$ are outside the initial boundary $\mathcal{B}$. Hence, in the final demapping (and encoder inverse) step, these outliers have to be projected back to the initial constellation. This is illustrated in

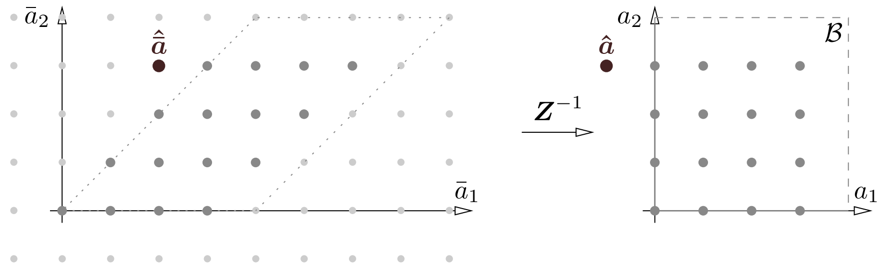

Figure C.5: Action of the inverse integer matrix on the decoding result.

Fig. C.5. The set $\mathbb{Z}^2$, w.r.t. which (in this illustration) decoding is done is shown in light gray; the decoding results as the dark bigger point.

In the above example $\boldsymbol{Z}$ was a unimodular matrix, i.e., $\det(\boldsymbol{Z}) = 1$. Consequently, $\boldsymbol{Z}\mathbb{Z}^2 = \mathbb{Z}^2$ and the valid points $\bar{\boldsymbol{a}}$ are a compact subset of $\mathbb{Z}^2$. This changes if $\det(\boldsymbol{Z}) > 1$; then the points $\bar{\boldsymbol{a}}$ are taken from a sub-lattice. This is illustrated in Fig. C.6 for $\boldsymbol{Z} = \begin{bmatrix} 1 & 1 \\ -1 & 1 \end{bmatrix}$. Since $\det(\boldsymbol{Z}) = 2$ the initial lattice is inflated by the factor 2 (and rotated by 45°) such that only every other point (checkerboard lattice) is a valid point for the integer linear combinations $\bar{\boldsymbol{a}}$.

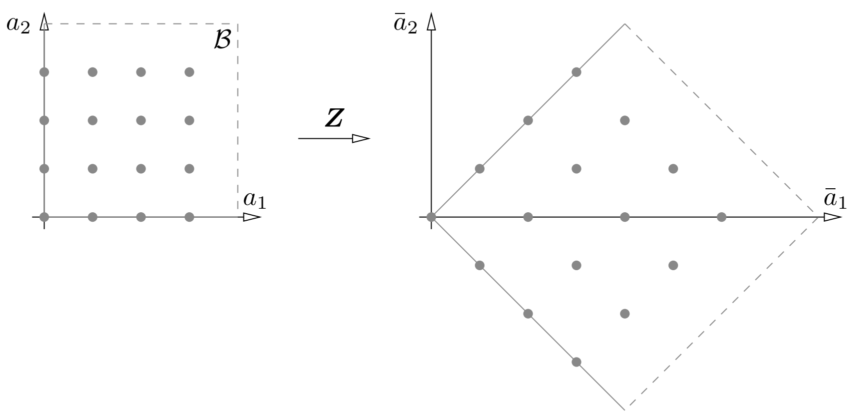

Figure C.6: Action of the integer matrix $\boldsymbol{Z} = \begin{bmatrix} 1 & 1 \\ -1 & 1 \end{bmatrix}$ on the data vectors $\boldsymbol{a} \in \mathbb{Z}_4^2$.

Now, due to individual decoding of the components, non-valid vectors interlaced between the valid one can be produced, see Fig. C.7. Since the inverse integer matrix reads $\boldsymbol{Z}^{-1} = \left[\begin{smallmatrix} .5 & -.5 \\ .5 & .5 \end{smallmatrix}\right]$ and $\det(\boldsymbol{Z}^{-1}) = \frac{1}{2}$, all points are shrunk by the factor $\frac{1}{2}$ (and rotated back). As as consequence, the decoding result $\hat{\boldsymbol{a}}$ is neither a valid point $\boldsymbol{a} \in \mathbb{Z}_4^2$ nor even taken from the lattice $\mathbb{Z}^2$. Again, the final demapping step has to take this fact into account and perform some suited quantization to the actual constellation.

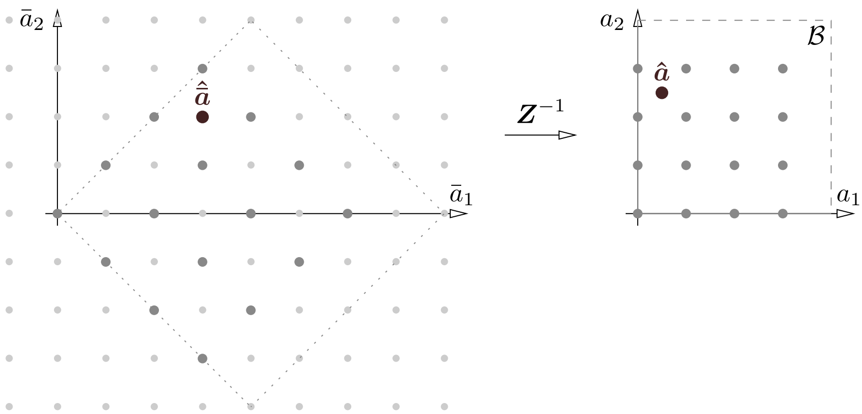

Figure C.7: Action of the inverse integer matrix on the decoding result.

Noteworthy, for sufficiently large SNR the probability for decoding results outside the transformed constellation is very small, but only asymptotically this effect becomes irrelevant.

D

Notation

This monograph uses standard mathematical notation. Scalar variables are typeset in italic lowercase letter, constants in Roman. Boldface lowercase letter denote vectors and boldface uppercase letters matrices.

Since the interaction between the real/complex field and finite fields is one of the key points, throughout the exposition the notation clearly distinguishes quantities over the real/complex numbers and over finite fields. The former are typeset in the conventional font (x, $\boldsymbol{x}$, $\boldsymbol{Z}$, $\dots$), whereas finite-field variables are typeset in Fraktur font ($\mathfrak{q}$, $\boldsymbol{\mathfrak{c}}$, $\boldsymbol{\mathfrak{Z}}_0$, $\dots$).

Sets:

Symbol	Meaning
$\mathbb{N}$	set of natural numbers (including 0)
$\mathbb{Z}$	set of integers
$\mathbb{G}$	set of Gaussian integers; $\mathbb{G} = \mathbb{Z} + \mathrm{j}\mathbb{Z}$, $\mathrm{j}^2 = -1$
$\mathbb{R}$, $\mathbb{C}$	real and complex numbers
$\mathbb{F}_p$	finite field of cardinality p

Vectors and Matrices:

Symbol	Meaning
$\boldsymbol{x}$	column vector (over $\mathbb{C}$)
$\underline{\boldsymbol{x}}$	row vector (over $\mathbb{C}$)
$\mathfrak{q}$	row vector over $\mathbb{F}_q$
$\boldsymbol{X} = [\,x_{i,j}\,]$	matrix with elements $x_{i,j}$
$\boldsymbol{X}^{\mathsf{T}}$, $\boldsymbol{X}^{\mathsf{H}}$	transpose and Hermitian of $\boldsymbol{X}$
$\boldsymbol{X}^{-1}$	inverse of $\boldsymbol{X}$
$\boldsymbol{X}^{-\mathsf{H}}$	Hermitian of inverse of $\boldsymbol{X}$; $\boldsymbol{X}^{-\mathsf{H}} = (\boldsymbol{X}^{-1})^{\mathsf{H}} = (\boldsymbol{X}^{\mathsf{H}})^{-1}$
$\boldsymbol{X}^{+}$	Moore–Penrose pseudo inverse of $\boldsymbol{X}$
$\boldsymbol{I}$	Identity matrix
$\boldsymbol{\mathcal{X}}$	augmented matrix of $\boldsymbol{X}$; $\boldsymbol{\mathcal{X}} = \left[\begin{smallmatrix}\boldsymbol{X}\\ c\boldsymbol{I}\end{smallmatrix}\right]$
$\mathbf{diag}(\cdot)$	diagonal matrix with given elements
$\det(\cdot)$	determinant
$\mathrm{trace}(\cdot)$	trace

Operators and Functions:

Symbol	Meaning
$*$	convolution
$\delta(x)$	Dirac delta
$\oplus$, $\odot$	addition and multiplication over $\mathbb{F}_p$
$\lvert\cdot\rvert$	scalars: absolute value; sets: cardinality
$\lvert\lvert\cdot\rvert\rvert$	Euclidean norm
$\mathrm{E}\{\cdot\}$	expectation
$\lfloor x \rfloor$	rounding to the next smaller integer (floor operation)
$\lfloor x \rceil$	rounding to the nearest integer (ties resolved towards $-\infty$)
$\mathrm{rem}_B(x)$	remainder of $x \in \mathbb{R}$ w.r.t. $B \in \mathbb{R}$; $\mathrm{rem}_B(x) \overset{\text{def}}{=} x - B\lfloor x/B \rfloor$
$\mathrm{mod}_B(x)$	modulo w.r.t. $B \in \mathbb{R}$ or $\mathbb{C}$; $\mathrm{mod}_B(x) \overset{\text{def}}{=} x - B\lfloor (x\,B^*)/\lvert B\rvert^2 \rceil$
$\mathrm{mod}_B^{\mathbb{E}}(x)$	modulo w.r.t. the Eisenstein integers
$\mathrm{lsb}_\phi(x)$	lsb of x in the binary expansion w.r.t. ϕ; $\mathrm{lsb}_\phi(x) = \mathfrak{x}_0$ for $x = [\ldots\,\mathfrak{x}_2\,\mathfrak{x}_1\,\mathfrak{x}_0]_\phi$

Designators:

Symbol	Meaning
$\hat{\cdot}$	estimate
$\bar{\cdot}$	integer linear combination
$\ddot{\cdot}$	modulo $\boldsymbol{\Lambda}_\mathrm{b}$ reduced integer linear combination

Mapping Functions:

Symbol	Meaning
$\mathcal{M}$	mapping of binary information to signal points
ψ	mapping from the finite-field elements "0" and "1" to integers "0" and "1"; $\psi(0) = 0$ and $\psi(1) = 1$
ϕ	base of the binary expansion of the signal points
Ψ	homomorphism between the arithmetics over the Gaussian integers modulo $\boldsymbol{\Lambda}_\mathrm{b}$ and that of the finite field $\mathbb{F}_p$; $\Psi(a) = \mathcal{M}^{-1}(\mathrm{mod}_{\boldsymbol{\Lambda}_\mathrm{b}}(a))$

Lattices:

Variable	Meaning
$\boldsymbol{\Lambda}(\boldsymbol{G})$	lattice generated by the generator matrix $\boldsymbol{G}$
$\mathcal{R}_\mathrm{V}(\boldsymbol{\Lambda})$	Voronoi region of $\boldsymbol{\Lambda}$ (cf. (2.2))
$\mathrm{Q}_{\boldsymbol{\Lambda}}(\boldsymbol{x})$	quantization of $\boldsymbol{x}$ to the nearest (squared Euclidean distance) point from $\boldsymbol{\Lambda}$ (cf. (2.6))
$\mathrm{mod}_{\boldsymbol{\Lambda}_\mathrm{b}}(\boldsymbol{x})$	modulo lattice operation; $\mathrm{mod}_{\boldsymbol{\Lambda}_\mathrm{b}}(\boldsymbol{x}) = \boldsymbol{x} - \mathrm{Q}_{\boldsymbol{\Lambda}_\mathrm{b}}(\boldsymbol{x})$
$\boldsymbol{\Lambda}_\mathrm{a}/\boldsymbol{\Lambda}_\mathrm{b}$	lattice partition (decomposition of $\boldsymbol{\Lambda}_\mathrm{a}$ into the sub-lattice $\boldsymbol{\Lambda}_\mathrm{b}$ and its cosets)
$\lvert\boldsymbol{\Lambda}_\mathrm{a}/\boldsymbol{\Lambda}_\mathrm{b}\rvert$	depth of lattice partition (number of cosets including the sublattice)
$\mathcal{A} + \mathcal{B}$	sum of (finite or infinite) sets $\mathcal{A}$ and $\mathcal{B}$; $\mathcal{A} + \mathcal{B} \stackrel{\mathrm{def}}{=} \{a + b \mid a \in \mathcal{A},\, b \in \mathcal{B}\}$

Constellations and Related Lattices:

Variable	Meaning
$\mathcal{A}$	signal constellation
M	cardinality of $\mathcal{A}$; $M = \lvert\mathcal{A}\rvert$
$\mathcal{C}$	lattice code
$\boldsymbol{\Lambda}_{\mathrm{a}}$	signal-point lattice
$\boldsymbol{\Lambda}_{\mathrm{b}}$	boundary lattice
$\boldsymbol{\Lambda}_{\mathrm{c}}$	coding lattice
$\boldsymbol{\Lambda}_{\mathrm{s}}$	shaping lattice

E

List of Acronyms

Subsequently, the most relevant acronyms used in the monography are alphabetically listed.

Acronym	Meaning
ASK	amplitude-shift keying
BC	broadcast channel
BLAST	Bell Laboratories Layered Space-Time
DFE	decision-feedback equalization
GSO	Gram–Schmidt orthogonalization
HKZ	Hermite–Korkine–Zolotarev
IF	integer-forcing
IRA	irregular repeat-accumulate
LDPC	low-density parity-check
LE	linear equalization
LLL	Lenstra–Lenstra–Lovász
LLR	log-likelihood ratio
LPE	linear preequalization
LRA	lattice-reduction-aided

Acronym	Meaning
MAC	multiple-access channel
MIMO	multiple-input/multiple-output
Mk	Minkowski
MLC	multilevel coding
MLD	maximum-likelihood detection
MMSE	minimum mean-squared error
MMSE-DFE	MMSE decision-feedback equalization
MMSE-LE	MMSE linear equalization
MSD	multistage decoding
pdf	probability density function
SBP	shortest basis problem
SIC	successive interference cancellation
SIVP	shortest independent vector problem
SMP	successive minima problem
QAM	quadrature-amplitude modulation
SNR	signal-to-noise ratio
SQRD	sorted QR decomposition
RCoF	reverse compute-and-forward
THP	Tomlinson-Harashima precoding
ZF	zero-forcing
ZF-DFE	ZF decision-feedback equalization
ZF-LE	ZF linear equalization

Acknowledgements

We thank Dr. Christoph Windpassinger and Dr. Michael Cyran for joint work on LRA and IF schemes and many fruitful discussions. Moreover, we thank Dr. Clemens Stierstorfer for very careful proofreading.

References

[1] E. Agrell, T. Eriksson, A. Vardy, K. Zeger. Closest Point Search in Lattices. *IEEE Transactions on Information Theory*, Vol. 48, No. 8, pp. 2201–2214, Aug. 2002.

[2] R. Ahlswede. Multi-Way Communication Channels. In *International Symposium on Information Theory*, Tsahkadsor, Armenia, USSR, Sept. 1971.

[3] M. Ajtai. The Shortest Vector Problem in L_2 is NP-hard for Randomized Reductions. In *Thirtieth Annual ACM Symposium on Theory of Computing*, pp. 10–19, Dallas, Texas, USA, May 1998.

[4] A. Akhavi. The Optimal LLL Algorithm is Still Polynomial in Fixed Dimension. *Theoretical Computer Science* vol. 297, pp. 3–23, Mar. 2003.

[5] J. Benesty, Y. Huang, J. Chen. A Fast Recursive Algorithm for Optimum Sequential Signal Detection in a BLAST System. *IEEE Transactions on Signal Processing*, Vol. 51, No. 7, pp. 1722–1730, July 2003.

[6] M. Bossert. *Channel Coding for Telecommunications*. John Wiley & Sons Ltd, 1999.

[7] L. Bruderer, C. Studer, M. Wenk, D. Seethaler, A. Burg. VLSI Implementation of a Low-Complexity LLL Lattice Reduction Algorithm for MIMO Detection. In *IEEE International Symposium on Circuits and Systems*, Paris, France, pp. 3745–3748, May/June 2010.

[8] L. Bruderer, C. Senning, A. Burg. Low-Complexity Seysen's Algorithm Based Lattice-Reduction-Aided MIMO Detection for Hardware Implementations. In *44th Asilomar Conference on Signals, Systems and Computers*, pp. 1468–1472, Pacific Grove, USA, Nov. 2010.

[9] G. Caire, G. Taricco, E. Biglieri. Bit-Interleaved Coded Modulation. *IEEE Transactions on Information Theory*, vol. 44, no. 3, pp. 927–946, May 1998.

[10] J.W.S. Cassels. *An Introduction to the Geometry of Numbers*. Springer Berlin/Heidelberg, Reprint of the 1971 Edition, 1997.

[11] S H. Chae, M. Jang, S.K. Ahn, J. Park, C. Jeong. Multilevel Coding Scheme for Integer-Forcing MIMO Receivers With Binary Codes. *IEEE Transactions on Wireless Communications*, vol. 16, no. 8, pp. 5428–5441, Aug. 2017.

[12] P.R. Chevillat, E. Eleftheriou. Decoding of Trellis-Encoded Signals in the Presence of Intersymbol Interference and Noise. *IEEE Transactions on Communications*, vol. 37, no. 7, pp. 669–676, July 1989.

[13] J.M. Cioffi, G.P. Dudevoir, M.V. Eyuboğlu, G.D. Forney. MMSE Decision-Feedback Equalizers and Coding — Part I: Equalization Results, Part II: Coding Results. *IEEE Transactions on Communications*, vol. 43, no. 10, pp. 2582–2604, Oct. 1995.

[14] J.M. Cioffi, G.D. Forney. Canonical Packet Transmission on the ISI Channel with Gaussian Noise. In *IEEE Global Telecommunications Conference*, pp. 1405–1410, London, UK, Nov. 1996.

[15] J.H. Conway, R. Guy. *The Book of Numbers*, Springer Verlag, New York, Berlin, 1996.

[16] J.H. Conway, N.J.A. Sloane. *Sphere Packings, Lattices and Groups*. Springer Verlag, New York, Berlin, 3rd edition, 1999.

[17] M.H.M. Costa. Writing on Dirty Paper. *IEEE Transactions on Information Theory*, vol. 29, no. 5, pp. 439–441, May 1983.

[18] L. Costantini, B. Matuz, G. Liva, E. Paolini, M. Chiani. Non-Binary Protograph Low-Density Parity-Check Codes for Space Communications. *International Journal of Satellite Communications and Networking*, vol. 30, no. 2, pp. 43–51, March/April 2012.

[19] T.M. Cover. Broadcast Channels. *IEEE Transactions on Information Theory*, vol. 18, no. 1, pp. 2–14, Jan. 1972.

[20] T.M. Cover, J.A. Thomas. *Elements of Information Theory*. John Wiley & Sons, Inc., New York, 2nd edition, 2006.

[21] M.C. Davey, D.J.C. MacKay. Low Density Parity Check Codes over GF(q). In *IEEE Information Theory Workshop*, Killarney, Ireland, pp. 70–71, June 1998.

[22] D. Declercq, M. Fossorier. Decoding Algorithms for Nonbinary LDPC Codes over GF(q). *IEEE Transactions on Communications*, vol. 55, no. 4, pp. 633–643, April 2007.

[23] L. Ding, K. Kansanen, Y. Wang, J. Zhang. Exact SMP Algorithms for Integer Forcing Linear MIMO Receivers. *IEEE Transactions on Wireless Communications*, vol. 14, no. 12, pp. 6955–6966, Dec. 2015.

[24] L. Ding, Y. Wang, J. Zhang. Complex Minkowski Reduction and a Relaxation for Near-Optimal MIMO Linear Equalization. *IEEE Wireless Communications Letters*, vol. 6, no. 1, pp. 38–41, Feb. 2017.

[25] A. Duel-Hallen, C. Heegard. Delayed Decision-Feedback Sequence Estimation. *IEEE Transactions on Communications*, vol. 37, no. 5, pp. 428–436, May 1989.

[26] A. Duel-Hallen. A Family of Multiuser Decision-Feedback Detectors for Asynchronous Code-Division Multiple-Access Channels. *IEEE Transactions on Communications*, Vol. 43, No. 2/3/4, pp. 421–434, February/March/April 1995.

[27] U. Erez, R. Zamir. Achieving $\frac{1}{2}\log(1 + \mathrm{SNR})$ on the AWGN Channel with Lattice Encoding and Decoding. *IEEE Transactions on Information Theory*, vol. 50, no. 10, pp. 2293–2314, Oct. 2004.

[28] W. van Etten. Maximum Likelihood Receiver for Multiple Channel Transmission Systems. *IEEE Transactions on Communications*, vol. 24, no. 2, pp. 276–283, Feb. 1976.

[29] M.V. Eyuboğlu, S.U.H. Qureshi. Reduced-State Sequence Estimation with Set Partitioning and Decision Feedback. *IEEE Transactions on Communications*, vol. 36, no. 1, pp. 13–20, Jan. 1988.

[30] C. Feng. D. Silva, F.R. Kschischang. An Algebraic Approach to Physical-Layer Network Coding. *IEEE Transactions on Information Theory*, vol. 59, no. 11, pp. 7576–7596, Nov. 2013.

[31] R.F.H. Fischer. *Precoding and Signal Shaping for Digital Transmission*, John Wiley & Sons, New York, 2002.

[32] R.F.H. Fischer, C. Windpassinger. Real- vs. Complex-Valued Equalisation in V-BLAST Systems. *IET Electronics Letters*, vol. 39, no. 5, pp. 470–471, March 2003.

[33] R.F.H. Fischer, J.B. Huber. Signal Processing in Receivers for Communication over MIMO ISI Channels. In *IEEE International Symposium on Signal Processing and Information Technology*, pp. 298–301, Darmstadt, Germany, Dec. 2003.

[34] R.F.H. Fischer. The Modulo-Lattice Channel: The Key Feature in Precoding Schemes. *AEÜ – International Journal of Electronics and Communications*, vol. 59, no. 4, pp. 244–253, June 2005.

[35] R.F.H. Fischer, C. Siegl. Lattice-Reduction-Aided Equalization for Transmission over Intersymbol-Interference Channels. *IET Electronics Letters*, vol. 41, pp. 969–970, Aug. 2005.

[36] R.F.H. Fischer, C. Siegl. On the Relation between Lattice-Reduction-Aided Equalization and Partial-Response Signaling. In *2006 International Zurich Seminar on Communications*, Zurich, Switzerland, pp. 34–37, Feb. 2006.

[37] R.F.H. Fischer. Lattice-Reduction-Aided Equalization and Generalized Partial Response Signaling for Point-to-Point Transmission over Flat-Fading MIMO Channels. In *4th International Symposium on Turbo Codes in connection with the 6th International Conference on Source and Related Topics*, Munich, Germany, April 2006.

[38] R.F.H. Fischer. From Gram–Schmidt Orthogonalization via Sorting and Quantization to Lattice Reduction. In *Joint Workshop on Coding and Communications (JWCC)*, Santo Stefano Belbo, Italy, Oct. 2010.

[39] R.F.H. Fischer. Efficient Lattice-Reduction-Aided MMSE Decision-Feedback Equalization. In *International Conference on Acoustics, Speech and Signal Processing*, Prag, Czech Republic, May 2011.

[40] R.F.H. Fischer, C. Windpassinger, C. Stierstorfer, C. Siegl, A. Schenk, Ü. Abay. Lattice-Reduction-Aided MMSE Equalization and the Successive Estimation of Correlated Data. *AEÜ – International Journal of Electronics and Communications*, vol. 65, no. 8, pp. 688–693, Aug. 2011.

[41] R.F.H. Fischer, M. Cyran, S. Stern, J.B. Huber. Modulo-Type Precoding for Networks. *Communications in Interference Limited Networks*, Springer Verlag, Berlin Heidelberg, pp. 31–52, Feb. 2016.

[42] R.F.H. Fischer, M. Cyran, S. Stern. Factorization Approaches in Lattice-Reduction-Aided and Integer-Forcing Equalization. In *2016 International Zurich Seminar on Communications*, Zurich, Switzerland, March 2016.

[43] R.F.H. Fischer, J.B. Huber, S. Stern, P. Guter. Multilevel Codes in Lattice-Reduction-Aided Equalization. In *2018 International Zurich Seminar on Communications*, Zurich, Switzerland, Feb. 2018.

[44] G.D. Forney. Coset Codes. I. Introduction and Geometrical Classification. *IEEE Trans. Information Theory*, vol. 34, no. 5, pp. 1123–1151, Sep. 1988.

[45] G.D. Forney. On the Role of MMSE Estimation in Approaching the Information-Theoretic Limits of Linear Gaussian Channels: Shannon meets Wiener. In *41st Allerton Conference on Communication, Control and Computing*, pp. 430–439, Monticello, IL, USA, Oct. 2003.

[46] G.J. Foschini. Layered Space-Time Architecture for Wireless Communication in a Fading Environment When Using Multiple Antennas. *Bell Laboratories Technical Journal*, vol. 1, no. 2, pp. 41–59, Autumn 1996.

[47] G.J. Foschini, D. Chizhik, M.J. Gans, C.Papadias, R.A. Valenzuela. Analysis and Performance of Some Basic Space-Time Architectures. *IEEE Journal on Selected Areas in Communications*, vol. 21, no. 3, pp. 303–320, Apr. 2003.

[48] Y.H. Gan, C. Ling, W.H. Mow. Complex Lattice Reduction Algorithm for Low-Complexity Full-Diversity MIMO Detection. *IEEE Transactions on Signal Processing*, vol. 57, pp. 2701–2710, July 2009.

[49] J. v.z. Gathen, J. Gerhard. *Modern Computer Algebra*. Cambridge University Press, Cambridge, UK, 2nd edition, 2002.

[50] W.J. Gilbert. Arithmetic in Complex Bases. *Mathematics Magazine*, vol. 57, No. 2, pp. 77–81, March 1984.

[51] G. Ginis, J.M. Cioffi. On the Relation Between V-BLAST and the GDFE. *IEEE Communications Letters*, vol. 5, no. 9, pp. 364–366, Sept. 2001.

[52] G.D. Golden, G.J. Foschini, R.A. Valenzuela, P.W. Wolniansky. Detection Algorithm and Initial Laboratory Results Using V-BLAST Space-Time Communication Architecture. *Electronics Letters*, Vol. 35, No. 1, pp. 14–15, Jan. 1999.

[53] G.H. Golub, C.F. van Loan. *Matrix Computations*, The Johns Hopkins University Press, Baltimore, third edition, 1996.

[54] R.M. Gray, D.L. Neuhoff. Quantization. *IEEE Transactions on Information Theory*, vol. 44, no. 6, pp. 2325–2383, Oct. 1998.

[55] B. Hassibi. An Efficient Square-Root Algorithm for BLAST. In *IEEE International Conference on Acoustics, Speech, and Signal Processing* pp. 737–740, Istanbul, Turkey, June 2000.

[56] W. He, B. Nazer, S. Shamai. Uplink-Downlink Duality for Integer-Forcing. In *IEEE International Symposium on Information Theory*, Honolulu, HI, USA, pp. 2544–2548, July 2014,

[57] W. He, B. Nazer, S. Shamai. Uplink-Downlink Duality for Integer-Forcing. *IEEE Transactions on Information Theory*, vol. 64, no. 3, pp. 1992–2011, March 2018.

[58] H. Harashima, H. Miyakawa. Matched-Transmission Technique for Channels with Intersymbol Interference. *IEEE Transactions on Communications*, vol. 20, no. 4, pp. 774–780, Aug. 1972.

[59] C. Hermite. Extraits de lettres de M.Ch. Hermite à M. Jacobi sur différents objects de la théorie des nombres. *Journal für die reine und angewandte Mathematik*, vol. 40, pp. 261–277, 1850.

[60] B. Hern, K.R. Narayanan. Multilevel Coding Schemes for Compute-and-Forward With Flexible Decoding. *IEEE Transactions on Information Theory*, vol. 59, no. 11, pp. 7613–7631, Nov. 2013.

[61] S.-N. Hong, G. Caire. Quantized Compute and Forward: A Low-Complexity Architecture for Distributed Antenna Systems. In *IEEE Information Theory Workshop*, pp. 420–424, Paraty, Brazil, Oct. 2011.

[62] S.-N. Hong, G. Caire. Compute-and-Forward Strategies for Cooperative Distributed Antenna Systems. *IEEE Transactions on Information Theory*, vol. 59, no. 9, pp. 5227–5243, Sep. 2013.

[63] R.A. Horn, C.R. Johnson. *Matrix Analysis*. Cambridge University Press, Cambridge, UK. Second edition, 2013.

[64] M.L. Honig and D.G. Messerschmitt. *Adaptive Filters–Structures, Algorithms, and Applications*. Kluwer Academic Publishers, Boston, 3. printing, 1985.

[65] Y.-C. Huang, K.R. Narayanan. Multistage Compute-and-Forward with Multilevel Lattice Codes Based on Product Constructions. In *2014 IEEE International Symposium on Information Theory (ISIT)*, pp. 2112–2116, June 29–July 4 2014.

[66] J. Huang, L. Yang, T. Yang, J. An. Design of Non-Binary Irregular Repeat-Accumulate Codes for Reliable Physical-Layer Network Coding. In *22nd International Conference on Telecommunications*, pp. 265–271, Sydney, Australia, Apr. 2015.

[67] Y. Huang, K.R. Narayanan, P. Wang. Lattices Over Algebraic Integers With an Application to Compute-and-Forward. *IEEE Transactions on Information Theory*, vol. 64, no. 10, pp. 6863–6877, Oct. 2018.

[68] J. Huber, W. Liu. An Alternative Approach to Reduced-Complexity CPM-Receivers. *IEEE Journal on Selected Areas in Communications*, vol. 7, no. 9, pp. 1437–1449, Dec. 1989.

[69] K. Huber. Codes over Gaussian Integers. *IEEE Transactions on Information Theory*, vol. 40, no. 1, pp. 207–216, Jan. 1994.

[70] H. Imai, S. Hirakawa. A New Multilevel Coding Method Using Error Correcting Codes. *IEEE Transactions on Information Theory*, vol. 23, no. 3, pp. 371–377, May 1977.

[71] R. Irmer, H. Droste, P. Marsch, M. Grieger, G. Fettweis, S. Brueck, H.P. Mayer, L. Thiele, V. Jungnickel. Coordinated Multipoint: Concepts, Performance, and Field Trial Results. *IEEE Communications Magazine*, vol. 49, no. 2, pp. 102–111, Feb. 2011.

[72] H. Jiang, S. Du. Complex Korkine-Zolotareff Reduction Algorithm for Full-Diversity MIMO Detection. *IEEE Communications Letters*, vol. 17, no. 2, pp. 381–384, Feb. 2013.

[73] H. Jin, A. Khandekar, R. McEliece. Irregular Repeat-Accumulate Codes. In *2nd International Symposium on Turbo Codes and Related Topics*, Brest, France, Sep. 2000.

[74] N. Jindal, S. Vishwanath, A.J. Goldsmith. On the Duality of Gaussian Multiple-Access and Broadcast Channels. *IEEE Transactions on Information Theory*, vol. 50, no. 4, pp. 768–783, April 2004.

[75] A. Kaye, D. George. Transmission of Multiplexed PAM Signals Over Multiple Channel and Diversity Systems. *IEEE Transactions on Communication Technology*, vol. 18, no. 5, pp. 520–526, Oct. 1970.

[76] A. Korkine, G. Zolotarev. Sur les formes quadratiques. *Mathematische Annalen*, vol. 6, pp. 366–389, 1873.

[77] J.C. Lagarias, H.W. Lenstra, C.P. Schnorr. Korkin-Zolotarev Bases and Successive Minima of a Lattice and its Reciprocal Lattice. *Combinatorica*, vol. 10, no. 4, pp. 333–348, 1990.

[78] A.K. Lenstra, H.W. Lenstra, L. Lovász. Factoring Polynomials with Rational Coefficients, *Mathematische Annalen*, vol. 261, no. 4, pp. 515–534, 1982.

[79] H. Liao. A Coding Theorem for Multiple Access communications. In *International Symposium on Information Theory*, Asilomar, CA, 1972.

[80] S. Lin, S. Song, L. Lan, L. Zeng, Y.Y. Tai. Constructions of Nonbinary Quasi-Cyclic LDPC Codes: A Finite Field Approach. *IEEE Transactions on Communications*, vol. 56, no. 4, pp. 545–554, Apr. 2008.

[81] C. Ling, L. Gan, W.H. Mow. A Dual-Lattice View of V-BLAST Detection. In *IEEE Information Theory Workshop*, pp. 478–482, Chengdu, China, 2006.

[82] C. Ling, W.H. Mow. A Unified View of Sorting in Lattice Reduction: From V-BLAST to LLL and Beyond. *IEEE Information Theory Workshop*, pp. 529–533, Taorminy, Italy, Oct. 2009.

[83] C. Ling, W.H. Mow, N. Howgrave-Graham. Reduced and Fixed-Complexity Variants of the LLL Algorithm for Communications. *IEEE Transactions on Communications*, vol. 61, no. 3, pp. 1040–1050, Mar. 2013. See also `arxiv.org/abs/1006.1661`, submitted on 8. Jun. 2010.

[84] C. Ling, J.C. Belfiore. Achieving AWGN Channel Capacity With Lattice Gaussian Coding. *IEEE Transactions on Information Theory*, vol. 60, no. 10, pp. 5918–5929, Oct. 2014.

[85] S. Lyu, C. Ling. Boosted KZ and LLL Algorithms. *IEEE Transactions on Signal Processing*, vol. 65, no. 18, pp. 4784–4796, Sept. 2017.

[86] H. Minkowski. Über die positiven quadratischen Formen und über kettenbruchähnliche Algorithmen. *Journal für die reine und angewandte Mathematik*, vol. 107, pp. 278–297, 1891.

[87] A.D. Murugan, H. El Gamal, M.O. Damen, G. Caire. A Unified Framework for Tree Search Decoding: Rediscovering the Sequential Decoder. *IEEE Transactions on Information Theory*, vol. 53, no. 3, pp. 933–953, Mar. 2006.

[88] B. Nazer, M. Gastpar. Compute-and-Forward: Harnessing Interference Through Structured Codes. *IEEE Transactions on Information Theory*, vol. 57, no. 10, pp. 6463–6486, Oct. 2011.

[89] B. Nazer, V.R. Cadambe, V. Ntranos, G. Caire. Expanding the Compute-and-Forward Framework: Unequal Powers, Signal Levels, and Multiple Linear Combinations. *IEEE Transactions on Information Theory*, vol. 62, no. 9, pp. 4879–4909, Sep. 2016.

[90] A.M. Nielsen, P. Kornerup. Redundant Radix Representations of Rings. *IEEE Transactions on Computers*, vol. 48, no. 11, pp. 1153–1165, Nov. 1999.

[91] W. Kositwattanarerk, F. Oggier. Connections Between Construction D and Related Constructions of Lattices. *Designs, Codes and Cryptography*, vol. 73, no. 2, pp. 441–455, Nov. 2014.

[92] O. Ordentlich, U. Erez. Achieving the Gains Promised by Integer-Forcing Equalization with Binary Codes. In *IEEE 26th Convention of Electrical and Electronics Engineers in Israel (IEEEI)*, pp. 000703–000707, 17.–20. Nov. 2010.

[93] O. Ordentlich, U. Erez. Cyclic-Coded Integer-Forcing Equalization. *IEEE Transactions on Information Theory*, vol. 58, no. 9, pp. 5804–5815, Sept. 2012.

[94] O. Ordentlich, U. Erez, B. Nazer. Successive Integer-Forcing and its Sum-Rate Optimality. *51st Annual Allerton Conference on Communication, Control, and Computing*, pp. 282–292, 2-4 Oct. 2013.

[95] O. Ordentlich, U. Erez, B. Nazer. The Approximate Sum Capacity of the Symmetric Gaussian K-User Interference Channel. *IEEE Transactions on Information Theory*, vol. 60, no. 6, pp. 3450–3482, June 2014.

[96] O. Ordentlich, U. Erez. Integer-Forcing Source Coding. In *2014 IEEE International Symposium on Information Theory (ISIT)*, pp. 181–185, June 29–July 4 2014.

[97] W. Penney. A "Binary" System for Complex Numbers. *Journal of the Association for Computing Machinery (JACM)*, vol. 12, no. 2, pp. 247–248, Apr. 1965.

[98] C. Poulliat, M. Fossorier, D. Declercq. Design of Regular (2,dc)-LDPC codes over GF(q) using their Binary Images. *IEEE Transactions on Communications*, vol. 56, no. 10, pp. 1626–1635, Oct. 2008.

[99] R. Price. Nonlinear Feedback Equalized PAM versus Capacity for Noisy Filter Channels. In *IEEE International Conference on Communications*, pp. 22.12–22.17, Philadelphia, PA, USA, June 1972.

[100] J.G. Proakis. *Digital Communications*. McGraw-Hill, New York, 2001.

[101] S.S. Ryshkov. The Theory of Hermite-Minkowski Reduction of Positive Definite Quadratic Forms. *Journal of Soviet Mathematics*, vol. 6, no. 6, pp. 651–671, Dec. 1976.

[102] A. Sakzad, J. Harshan, E. Viterbo. On Complex LLL Algorithm for Integer Forcing Linear Receivers. In *2013 Australian Communications Theory Workshop (AusCTW)*, pp. 13–17, Jan. 29–Feb. 1, 2013.

[103] A. Sakzad, J. Harshan, E. Viterbo. Integer-Forcing MIMO Linear Receivers Based on Lattice Reduction. *IEEE Transactions on Wireless Communications*, vol. 12, no. 10, pp. 4905–4915, Oct. 2013.

[104] J. Salz. Digital Transmission over Cross-Coupled Linear Channels. *AT&T Technical Journal*, vol. 64, no. 6, pp. 1147–1159, July–Aug. 1985.

[105] A.H. Sayed. *Fundamentals of Adaptive Filtering*, John Wiley & Sons, New York, 2003.

[106] D.A. Schmidt, M. Joham, W. Utschick. Minimum Mean Square Error Vector Precoding. *European Transactions on Telecommunications*, vol. 19, no. 3, pp. 219–231, Apr. 2008.

[107] C.P. Schnorr, M. Euchner. Lattice Basis Reduction: Improved Practical Algorithms and Solving Subset Sum Problems. *Mathematical Programming*, pp. 181–199, 1994.

[108] M. Schubert, H. Boche. A Unifying Theory for Uplink and Downlink Multi-User Beamforming. In *2002 International Zurich Seminar on Communications*, pp. 27/1–27/6, Zurich, Switzerland, Feb. 2002.

[109] S. Shamai, B.M. Zaidel. Enhancing the Cellular Downlink Capacity via Co-processing at the Transmitting End. In *IEE Vehicular Technology Conference, Spring 2001*, Rhodes, Greece, pp. 1745–1749, May 2001.

[110] C.E. Shannon. A Mathematical Theory of Communication. *Bell System Technical Journal*, pt. I, vol. 27, no. 3, pp. 379–423, July 1948; pt. II, vol. 27, no. 4, pp. 623–656, Oct. 1948.

[111] M. Seysen. Simultaneous Reduction of a Lattice Basis and its Reciprocal Basis. *Combinatorica*, vol. 13, no, 3, pp. 363–376, Sept. 1993.

[112] C.L. Siegel. *Lectures on the Geometry of Numbers.* Springer Verlag, Berlin, Germany, 1989.

[113] S. Stern, R.F.H. Fischer. Lattice-Reduction-Aided Preequalization over Algebraic Signal Constellations. In *9th International Conference on Signal Processing and Communication Systems (ICSPCS)*, Cairns, Australia, Dec. 2015.

[114] S. Stern, R.F.H. Fischer. Joint Algebraic Coded Modulation and Lattice-Reduction-Aided Preequalization. *Electronic Letters*, vol. 52, no. 7, pp. 523–525, March 2016

[115] S. Stern, R.F.H. Fischer. Lattice-Reduction-Aided Precoding for Coded Modulation over Algebraic Signal Constellations. In *20th International ITG Workshop on Smart Antennas*, pp. 356–363, Munich, Germany, Mar. 2016.

[116] S. Stern, R.F.H. Fischer. Optimal Factorization in Lattice-Reduction-Aided and Integer-Forcing Linear Equalization. In *11. Int. ITG Conf. on Systems, Communications, and Coding (SCC)*, Hamburg, Germany, February 2017

[117] S. Stern, R.F.H. Fischer. V-BLAST in Lattice Reduction and Integer Forcing. In *2017 IEEE International Symposium on Information Theory (ISIT)*, Aachen, Germany, July 2017.

[118] S. Stern, D. Rohweder, J. Freudenberger, R.F.H. Fischer. Binary Multilevel Coding over Eisenstein Integers for MIMO Broadcast Transmission. In *23th International ITG Workshop on Smart Antennas*, Vienna, Austria, Apr. 2019.

[119] C. Stierstorfer, R.F.H. Fischer. Lattice-Reduction-Aided Tomlinson-Harashima Precoding for Point-to-Multipoint Transmission. *AEÜ – International Journal of Electronics and Communications*, vol. 60, pp. 328–330, April 2006.

[120] Q.T. Sun, J. Yuan, T. Huang, K.W. Shum. Lattice Network Codes Based on Eisenstein Integers. *IEEE Transactions on Communications*, vol. 61, no. 7, pp. 2713–2725, July 2013.

[121] M. Taherzadeh, A. Mobasher, A. K. Khandani. LLL Lattice-Basis Reduction Achieves the Maximum Diversity in MIMO Systems. In *International Symposium on Information Theory*, pp. 1300–1304, Sep. 2005.

[122] M. Taherzadeh, A. Mobasher, A.K. Khandani. LLL Reduction Achieves the Receive Diversity in MIMO Decoding. *IEEE Transactions on Information Theory*, vol. 53, no. 12, pp. 4801–4805, Dec. 2007.

[123] M. Tanahashi, H. Ochiai. A Multilevel Coded Modulation Approach for Hexagonal Signal Constellation. *IEEE Transactions on Wireless Communications*, vol. 8, no. 10, pp. 4993–4997, Oct. 2009.

[124] E. Telatar. Capacity of Multi-Antenna Gaussian Channels. *European Transactions on Telecommunications*, vol. 10, no. 6, pp. 585–596, Nov. 1999.

[125] M. Tomlinson. New Automatic Equaliser Employing Modulo Arithmetic. *Electronics Letters*, vol. 7, no. 5, pp. 138–139, March 1971.

[126] H.L. van Trees. *Detection, Estimation, and Modulation Theory—Part III: Radar-Sonar Signal Processing and Gaussian Signals in Noise*. John Wiley & Sons, Inc., New York, 1971.

[127] D. Tse, P. Viswanath. *Fundamentals of Wireless Communication*. Cambridge Universty Press, Cambridge, UK, 2005.

[128] N.E. Tunali, Y.C. Huang, J.J. Boutros, K.R. Narayanan. *Lattices over Eisenstein Integers for Compute-and-Forward. IEEE Transactions on Information Theory*, vol. 61, no. 10, pp. 5306–5321, Oct. 2015.

[129] G. Ungerböck. Channel Coding with Multilevel/Phase Signals. *IEEE Transactions on Information Theory*, vol. 28, no. 1, pp. 55–67, Jan. 1982.

[130] P. Viswanath, D.N. Tse. Sum Capacity of the Vector Gaussian Broadcast Channel and Uplink-Downlink Duality. *IEEE Transactions on Information Theory*, vol. 49, no. 8, pp. 1912–1921, Aug. 2003.

[131] S. Vishwanath, N. Jindal, A. Goldsmith. Duality, Achievable Rates, and Sum-Rate Capacity of Gaussian MIMO Broadcast Channels. *IEEE Transactions on Information Theory*, vol. 49, no. 10, pp. 2658–2668, Oct. 2003.

[132] A.J. Viterbi. *CDMA: Principles of Spread Spectrum Communications*. Addison-Wesley, Reading, MA, USA, 1995.

[133] A.J. Viterbi. An Intuitive Justification and a Simplified Implementation of the MAP Decoder for Convolutional Codes. *IEEE Journal on Selected Areas in Communications*, vol. 16, no. 2, pp. 260–264, Feb. 1998.

[134] U. Wachsmann, R.F.H. Fischer, J.B. Huber. Multilevel Codes: Theoretical Concepts and Practical Design Rules. *IEEE Transactions on Information Theory*, vol. 45, no. 5, pp. 1361–1391, Jul 1999.

[135] L. Wei, W. Chen. Integer-Forcing Linear Receiver Design over MIMO Channels. In *IEEE Global Communications Conference (GLOBECOM)*, Anaheim, CA, pp. 3560–3565, Dec. 2012.

[136] L. Wei, W. Chen. Integer-Forcing Linear Receiver Design with Slowest Descent Method. in *IEEE Transactions on Wireless Communications*, vol. 12, no. 6, pp. 2788–2796, June 2013.

[137] J. Wen, L. Li, X. Tang, W.H. Mow, C. Tellambura. An Efficient Optimal Algorithm for Integer-Forcing Linear MIMO Receivers Design. In *IEEE International Conference on Communications (ICC)*, Paris, France, May 2017.

[138] J. Wen, X. Chang. On the KZ Reduction. *IEEE Transactions on Information Theory*, vol. 65, no. 3, pp. 1921–1935, March 2019.

[139] C. Windpassinger, R.F.H. Fischer. Low-Complexity Near-Maximum-Likelihood Detection and Precoding for MIMO Systems using Lattice Reduction. In *IEEE Information Theory Workshop*, pp. 345–348, Paris, France, March/April 2003.

[140] C. Windpassinger, R.F.H. Fischer. Optimum and Sub-Optimum Lattice-Reduction-Aided Detection and Precoding for MIMO Communications. In *Canadian Workshop on Information Theory*, pp. 88–91, Waterloo, Ontario, Canada, May 2003.

[141] C. Windpassinger, R.F.H. Fischer, T. Vencel, J.B. Huber. Precoding in Multi-Antenna and Multi-User Communications. *IEEE Transactions on Wireless Communications*, vol. 3, no. 4, pp. 1305–1316, June 2004.

[142] C. Windpassinger. *Detection and Precoding for Multiple Input Multiple Output Channels*. Dissertation, University Erlangen–Nürnberg, June 2004.

[143] C. Windpassinger, R.F.H. Fischer, J.B. Huber. Lattice-Reduction-Aided Broadcast Precoding. *IEEE Transactions on Communications*, vol. 52, no. 12, pp. 2057–2060, Dec. 2004.

[144] P. Wolniansky, G. Foschini, G. Golden, R. Valenzuela. V-BLAST: An Architecture for Realizing Very High Data Rates Over the Rich-Scattering Wireless Channel. In *1998 URSI International Symposium on Signals, Systems, and Electronics*, Pisa, Italy, Oct. 1998.

[145] D. Wübben, R. Böhnke, V. Kühn, K.D. Kammeyer. MMSE Extension of V-BLAST Based on Sorted QR Decomposition. In *IEEE Vehicular Technology Conference*, pp. 508–512, Orlando, Florida, USA, Oct. 2003.

[146] D. Wübben, R. Böhnke, V. Kühn, K.D. Kammeyer. Near-Maximum-Likelihood Detection of MIMO Systems using MMSE-Based Lattice Reduction. *IEEE International Conference on Communications*, pp. 798–802, Paris, France, June 2004.

[147] D. Wübben, D. Seethaler. On the Performance of Lattice Reduction Schemes for MIMO Data Detection. In *41st Asilomar Conference on Signals, Systems and Computers*, pp. 1534–1538, Pacific Grove, USA, Nov. 2007.

[148] D. Wübben, D. Seethaler, J. Jalden, G. Matz. Lattice Reduction. *IEEE Signal Processing Magazine*, vol. 28, no. 3, pp. 70–91, May 2011.

[149] J. Yang, S. Roy. Joint Transmitter-Receiver Optimization for Multi-Input Multi-Output Systems with Decision Feedback. *IEEE Transactions on Information Theory*, vol. 40, no. 5, pp. 1334–1347, Sep. 1994.

[150] Y. Yang, C. Chen, J. Mu, J. Wang. Nonbinary Quasi-Cyclic LDPC Cycle Codes with Low-Density Systematic Quasi-Cyclic Generator Matrices. *IEICE Transactions on Communications*, vol. E94.B, no. 9, pp. 2620–2623, Sep. 2011.

[151] H. Yao, G. Wornell. Lattice-Reduction-Aided Detectors for MIMO Communication Systems. In *Proceedings of IEEE Global Telecommunications Conference*, pp. 424–428, Taipei, Taiwan, Nov. 2002.

[152] W. Yu, J.M. Cioffi. Sum Capacity of Gaussian Vector Broadcast Channels. *IEEE Transactions on Information Theory*, vol. 50, no. 9, pp. 1875–1892, Sep. 2004.

[153] R. Zamir. *Lattice Coding for Signals and Networks*. Cambridge University Press, Cambridge, U.K. 2014.

[154] J. Zhan, B. Nazer, U. Erez, M. Gastpar. Integer-Forcing Linear Receivers. *IEEE Transactions on Information Theory*, vol. 60, no. 12, pp. 7661–7685, Dec. 2014.

[155] W. Zhang, S. Qiao, Y. Wei. HKZ and Minkowski Reduction Algorithms for Lattice-Reduction-Aided MIMO Detection. *IEEE Transactions on Signal Processing*. vol. 60, no. 11, pp. 5963–5976, Nov. 2012.